

Low-complexity iterative method for hybrid MPC[★]

Damian Frick^a, Juan L. Jerez^{a,b}, Alexander Domahidi^{b,c}, Angelos Georghiou^d,
Manfred Morari^a

^a*Automatic Control Laboratory, ETH Zürich, Physikstrasse 3, 8092 Zürich, Switzerland*

^b*embotech GmbH, Physikstrasse 3, 8092 Zürich, Switzerland*

^c*inspire AG, Technoparkstrasse 1, 8005 Zürich, Switzerland*

^d*Desautels Faculty of Management, McGill University, Montreal, Quebec, Canada*

Abstract

Model predictive control problems for constrained hybrid systems are usually cast as mixed-integer optimization problems (MIP). However, commercial MIP solvers are designed to run on desktop computing platforms and are not suited for embedded applications which are typically restricted by limited computational power and memory. To alleviate these restrictions, we develop a novel low-complexity, iterative method for a class of non-convex, non-smooth optimization problems. This class of problems encompasses hybrid model predictive control problems where the dynamics are piece-wise affine (PWA). We give conditions under which the proposed algorithm has fixed points (existence of solutions) and show that, under practical assumptions, our method is guaranteed to converge locally. This is in contrast to other low-complexity methods in the literature, such as the non-convex alternating directions method of multipliers (ADMM), that give no such guarantees for this class of problems. By interpreting the PWA dynamics as a union of polyhedra we can exploit the problem structure and develop an algorithm based on operator splitting procedures. Our algorithm departs from the traditional MIP formulation, and leads to a simple, embeddable method that only requires matrix-vector multiplications and small-scale projections onto polyhedra. We illustrate the efficacy of the method on two numerical examples, achieving performance close to the global optimum with computational times several orders of magnitude smaller compared to state-of-the-art MIP solvers.

Key words: Operator splitting; Hybrid model predictive control; Non-smooth and discontinuous problems; Iterative schemes.

1 Introduction

Many practical applications for control fall in the domain of hybrid systems, including applications such as traction control, active suspension control or energy management in automobiles [1–3], as well as applications in power electronics [4, 5]. These applications often require fast sampling times in the sub-second range, and the control algorithms need to be implemented on industrial, resource-constrained embedded platforms, such as microcontrollers or re-configurable hardware. Hybrid systems are characterized by complex interactions between discrete and continuous behaviors that make them extremely challenging to control. In most cases this requires complex application-specific rules that are subject to tuning. In the last decades receding horizon control and model predictive control (MPC) [6–8] have received widespread attention both in research and industry. These techniques provide a systematic approach for controlling constrained hybrid systems, promising high control performance with minimal tuning effort.

[★] This manuscript is the preprint of a paper submitted to Automatica and is subject to Elsevier copyright. Elsevier maintains the sole rights of distribution or publication of the work in all forms and media. If accepted, the copy of record will be available at <http://www.journals.elsevier.com/automatica/>.

Email addresses: dafrick@control.ee.ethz.ch (Damian Frick), juanj@control.ee.ethz.ch (Juan L. Jerez), domahidi@inspire.ethz.ch (Alexander Domahidi), angelos.georghiou@mcgill.ca (Angelos Georghiou), morari@control.ee.ethz.ch (Manfred Morari).

For many hybrid MPC problems, mature modeling software together with very efficient solvers are already available. The field has particularly benefited from the introduction of the mixed logical dynamical framework [9], which defines clear rules for formulating hybrid MPC as mixed-integer optimization problems (MIP), and the rise of powerful commercial solvers for general-purpose MIP, such as CPLEX [10] and Gurobi [11]. This has enabled control engineers to deploy hybrid MPC on desktop computing platforms. These software packages have focused on the solution of generic, large-scale, mixed-integer linear and quadratic programming (MIQP) problems on powerful computing platforms. This has several drawbacks: (i) their code size is in the order of tens of megabytes; (ii) the algorithms require substantial working memory, e.g. in some branch-and-bound methods; (iii) they depend on numerical libraries that cannot be ported to most embedded control platforms. This has restricted the applicability of hybrid MPC to systems such as the control of buildings [12, 13] or chemical processes [14] that can run on desktop computing platforms, with sampling times in the order of minutes or even hours.

Recently there have been various efforts to enable hybrid MPC applications with faster dynamics to run on platforms with more limited computational power. To achieve this, these methods exploit (i) the sparsity-inducing multistage structure of MPC problems, and (ii) the fact that MPC problems are formulated as parametric problems, and are solved in a receding horizon fashion, where the structure of the optimization problem remains static, with only few changing parts in the problem data. This motivates the development of (parametric) solvers that are tailored to specific MPC problems. In particular, methods based on MIP reformulations have been investigated and lead to reduced computation times compared to general-purpose solvers. For MPC and mixed-integer optimal control problems, algorithms such as those described in [15–18], have led to improvements to standard methods, such as branch-and-bound and branch-and-cut, by taking advantage of the problem structure. The structure and parametric nature of the problems has been exploited to generate stronger cuts, tighter relaxations, as well as tailored branching and rounding heuristics. Furthermore, code-generation has been used to generate tailored (parametric) subproblem solvers used in branch-and-bound. These methods are limited by the fact that they are based on enumeration and focus on finding global minima. Furthermore, they often rely on complex solvers to find solutions of relaxed problems.

Low-complexity methods based on operator splitting concepts, can overcome these issues, enabling the use of hybrid MPC on embedded platforms. These methods trade off computational complexity with optimality, i.e., they typically produce a “good” solution in a fraction of the time required by general-purpose, or even tailored MIP solvers, to find global optima. Furthermore, they allow the (potentially complex) optimization problem to be split into several, lower complexity, subproblems, making these methods especially suited for embedded applications and implementations on computing systems with highly limited resources. The alternating directions method of multipliers (ADMM) [19, 20] is an example of such an operator splitting method. It was used in [21] to exploit the structure of linear MPC problems, leading to a low-complexity, embedded implementation that could achieve solution times in the microsecond range. In [22], ADMM was used on various hybrid MPC examples achieving substantial gains in computational performance compared to general-purpose MIP solvers. Convergence guarantees are available for some special cases of non-convex ADMM [23, 24], however neither optimality or convergence guarantees are available for the case of hybrid MPC. Good examples for low-complexity methods that offer superior computational performance compared to conventional methods, while still retaining some guarantees on optimality and convergence, are [25, 26]. Both methods are using operator splitting techniques to exploit the structure of smooth, non-convex MPC problems, but do not address the, practically important, class of hybrid MPC problems considered here.

1.1 Contribution

In this paper, we develop an algorithm based on operator splitting to address hybrid MPC problems, that, in the spirit of [25, 26], provides both the desired theoretical guarantees, and computational speed. Our method exploits the multistage structure of the optimization problem, allowing to decompose the complex piece-wise affine (PWA) equality constraints into decoupled non-convex polyhedral constraints. By leveraging the polyhedral nature of these constraints, we are able to derive guarantees on optimality and convergence. The main contributions of this paper are the following:

- We propose an iterative, numerical method to find local minima of a class of non-convex, non-smooth optimization problems that arises in constrained optimal control problems for systems with PWA dynamics. Our method is of low complexity and only requires first-order information in the form of matrix-vector multiplications and small-scale Euclidean projections onto convex polyhedra.
- We provide (i) checkable conditions for the existence of fixed points of the proposed algorithm, (ii) show that the method converges locally to such fixed points and (iii) prove that fixed points correspond to local minima. To the author’s knowledge, for the class of problems considered, this is the first method of such simplicity that allows to give local optimality and convergence guarantees.

- The proposed algorithm is implemented using automatic code generation that does not require any additional numerical libraries and directly targets the embedded applications. This code generation tool is made publicly available via github [27]. We examine the performance of the method on two numerical examples, and demonstrate that the proposed method can achieve computational times several orders of magnitude faster than conventional MIQP solvers, with only a minor loss of optimality.

1.2 Outline

The remainder of the paper is organized as follows: In Section 2 we outline the problem statement, define an auxiliary problem called the *consensus problem* and show how an MPC problem with PWA dynamics can be transformed into such a canonical description. In Section 3, we construct an operator whose fixed points correspond to local minima of the problem. In Section 4, we propose an algorithm based on the operator, and discuss important properties of the method such as local optimality, existence of fixed points and local convergence. In Section 5, we present our numerical results. Proofs of most statements are presented in the appendix.

1.3 Notation & elementary definitions

For vectors $x, y \in \mathbb{R}^n$ the norm $\|x\| := \sqrt{x^\top x}$ denotes the 2-norm and the scalar product is defined as $\langle x, y \rangle := x^\top y$. Given a point x and a closed set \mathcal{C} , $\mathcal{P}_{\mathcal{C}}(x) := \arg \min_{z \in \mathcal{C}} \|x - z\|$ is the Euclidean projection of point x onto set \mathcal{C} . We denote the closed ϵ -ball around x by $\mathcal{B}_\epsilon(x) := \{z \mid \|x - z\| \leq \epsilon\}$ and we will use the shorthand $\mathcal{B}_\epsilon := \mathcal{B}_\epsilon(0)$. By $\mathcal{C} + \{x\}$ we denote the Minkowski sum of the set \mathcal{C} and the singleton x , i.e., \mathcal{C} is shifted by x . The *relative boundary* of a set \mathcal{C} is defined as $\text{relbd } \mathcal{C} := \text{cl } \mathcal{C} \setminus \text{relint } \mathcal{C}$, where $\text{cl } \mathcal{C}$ is the *closure* and $\text{relint } \mathcal{C}$ the *relative interior*. The *characteristic function* of a set \mathcal{C} is defined by $\chi_{\mathcal{C}}(x) := \{0 \text{ if } x \in \mathcal{C}; +\infty \text{ otherwise}\}$. An *operator* $T : \mathcal{X} \rightrightarrows \mathcal{Y}$ is a mapping that maps every point $x \in \mathcal{X}$ to a set $T(x) \subseteq \mathcal{Y}$. An operator T is called *single-valued* if for all $x \in \mathcal{X}$: $T(x)$ is a singleton. A *zero* of an operator is a point $x \in \mathcal{X}$ such that $0 \in T(x)$, this is denoted by $x \in \text{zero } T$, where $\text{zero } T := \{x \mid 0 \in T(x)\}$. A *fixed point* of an operator is a point $x \in \mathcal{X}$ such that $x \in T(x)$, this is denoted by $x \in \text{fix } T$, where $\text{fix } T := \{x \mid x \in T(x)\}$.

2 Problem statement

In this work, we consider MPC problems for systems described by PWA functions. The problems are *parametric*, i.e., only parts of the problem data will change every time the solver is invoked. In particular, we address problems, parameterized by $\theta \in \mathbb{R}^p$, with the following general structure:

$$p^*(\theta) := \min_{z \in \mathbb{R}^n} \quad \frac{1}{2} z^\top H z + h^\top z \quad (1a)$$

$$\text{s. t.} \quad z \in \mathcal{E} \cap \mathcal{Z}(\theta), \quad (1b)$$

with $H \in \mathbb{R}^{n \times n}$ positive definite, and $z := (z_1, \dots, z_N) \in \mathbb{R}^n$, with $z_k \in \mathbb{R}^{n_k}$. The non-convex set $\mathcal{Z}(\theta) \subseteq \mathbb{R}^n$ has the following form:

$$\mathcal{Z}(\theta) := \bigtimes_{k=1}^N \left(\bigcup_{i=1}^{m_k} \mathcal{Z}_{k,i}(\theta) \right), \quad (1c)$$

and the sets $\mathcal{Z}_{k,i}(\theta) \subseteq \mathbb{R}^{n_k}$ are closed convex polyhedra that may depend linearly on θ , in the following way:

$$\mathcal{Z}_{k,i}(\theta) := \{z_k \in \mathbb{R}^{n_k} \mid F_{k,i} z_k \leq f_{k,i}(\theta), G_{k,i} z_k = g_{k,i}(\theta)\}, \quad (1d)$$

with matrices and vectors of appropriate dimensions, and $f_{k,i}(\theta)$, $g_{k,i}(\theta)$ affine functions of the parameter θ . Note that the parameter θ could be further restricted to lie in a polyhedral set without loss of generality. For a given parameter θ , the Euclidean projection onto $\mathcal{Z}(\theta)$ can be evaluated very efficiently, by decoupling it into simple convex projections, as detailed in Section 4, Algorithm 2. This important feature of \mathcal{Z} will be a key ingredient to the algorithm presented in Section 4. For simplicity of notation we will omit the parameter dependence of $\mathcal{Z}(\theta)$ in the remainder of this paper and just refer to it as \mathcal{Z} . Whenever the parameter dependence becomes material we will consider it explicitly. Finally, the set \mathcal{E} is an affine equality constrained set

$$\mathcal{E} := \{z \in \mathbb{R}^n \mid Az = b\} \quad (1e)$$

$$= \{Vv + \bar{v} \mid v \in \mathbb{R}^{n-m}\}, \quad (1f)$$

with $A \in \mathbb{R}^{m \times n}$ full row rank. Equation (1f) is an alternative form of \mathcal{E} for an appropriate matrix $V \in \mathbb{R}^{n \times n-m}$ and vector $\bar{v} \in \mathbb{R}^m$ [28, p. 430, (15.14)], where V has full column rank by construction. To simplify notation, this alternative form will be used in the remainder of this paper. We furthermore assume that $\mathcal{E} \cap \mathcal{Z}$ is non-empty, hence the problem has a feasible solution.

2.1 Consensus form

Problem (1) can also be re-written in the so-called consensus form, by introducing copies y of z as follows

$$p^* := \min_{z,y} \frac{1}{2} z^\top H z + h^\top z + \chi_{\mathcal{E}}(z) + \chi_{\mathcal{Z}}(y) \quad (2a)$$

$$\text{s. t. } z = y. \quad (2b)$$

Problem (2) is a non-convex, non-smooth optimization problem. The constraint sets \mathcal{E} and \mathcal{Z} have been moved into the cost function, using their characteristic functions $\chi_{\mathcal{E}}(z)$ and $\chi_{\mathcal{Z}}(y)$. Note that this problem formulation ensures that the two sets \mathcal{E} and \mathcal{Z} can be decoupled, with the consensus constraint $z = y$ encoding the coupling between the original variables. This will be exploited in Section 4 to derive an efficient operator splitting method.

2.2 Model Predictive Control

We are particularly interested in MPC problems where the discrete dynamics are given, or can be approximated, by a PWA function of the states and inputs. Such parametric hybrid MPC problems can be written as:

$$\min_{x_k, u_k} \sum_{k=1}^N (x_{k+1} - \bar{x}_{k+1})^\top Q_{k+1} (x_{k+1} - \bar{x}_{k+1})^\top + (u_k - \bar{u}_k)^\top R_k (u_k - \bar{u}_k)^\top \quad (3a)$$

$$\text{s. t. } x_{k+1} = A_{k,i} x_k + B_{k,i} u_k + c_{k,i}, \text{ if } (x_k, u_k) \in \mathcal{C}_{k,i}, k = 1, \dots, N, \quad (3b)$$

$$x_1 = \theta,$$

for $i = 1, \dots, m_k$ with m_k representing the number of regions of the PWA dynamics. Vector $x_k \in \mathbb{R}^{n_x}$ denotes the state of the system at time k , $u_k \in \mathbb{R}^{n_u}$ denotes the inputs applied to the system between times k and $k + 1$, and $\theta \in \mathbb{R}^{n_x}$ is the (parametric) initial state of the system. The vectors \bar{x}_k and \bar{u}_k denote the state and input references at time k . The sets $\mathcal{C}_{k,i}$ are non-empty, closed, convex polyhedra that define the partition of the PWA dynamics, and include state and input constraints.

Problems of the form (3) can be solved by introducing additional continuous and binary variables, and formulating an MIQP using the big-M reformulation [9]. The resulting programs can be solved using powerful, commercial MIP solvers such as CPLEX [10], Gurobi [11] or MOSEK [29]. However, these solvers require substantial working memory, have large code size and typically suffer from severe computational performance degradation, when the horizon length N becomes large due to the linear growth in the number of binary variables with the prediction horizon N . These issues become a major limitation for embedded platforms.

Instead of formulating a MIP, in this work we transform Problem (3) into the form (1). In this way only Nn_x auxiliary continuous variables and *no binary variables* need to be introduced. In contrast, the big-M reformulation proposed in [9] requires $\sum_{k=1}^N m_k$ binary and $\sum_{k=1}^N m_k n_x$ continuous auxiliary variables. For each time instant k we introduce a copy w_k of x_{k+1} . This vector of auxiliary variables is defined as

$$w_k := A_{k,i} x_k + B_{k,i} u_k + c_{k,i}, \text{ for } (x_k, u_k) \in \mathcal{C}_{k,i},$$

and allows us to define the convex, polyhedral sets

$$\mathcal{Z}_{1,i}(\theta) := \{(u_1, w_1) \mid w_1 = A_{1,i} \theta + B_{1,i} u_1 + c_{1,i}, (\theta, u_1) \in \mathcal{C}_{1,i}\},$$

for $i = 1, \dots, m_1$, and

$$\mathcal{Z}_{k,i} := \{(x_k, u_k, w_k) \mid w_k = A_{k,i} x_k + B_{k,i} u_k + c_{k,i}, (x_k, u_k) \in \mathcal{C}_{k,i}\},$$

for $k = 2, \dots, N$ and $i = 1, \dots, m_k$. It should be noted that the sets $\mathcal{Z}_{k,i}$ are closed by construction. The non-convex constraint set \mathcal{Z} now has the form of (1c) and is *decoupled* in the horizon N . Finally, to have an equivalent formulation, we need to impose $x_{k+1} = w_k$. We define a set of *coupling* equality constraints

$$\mathcal{E} := \bigtimes_{k=1}^N (\mathbb{R}^{n_u} \times \mathcal{E}_k),$$

where, for any $k = 1, \dots, N$, we have that

$$\mathcal{E}_k := \{(w_k, x_{k+1}) \in \mathbb{R}^{2n_x} \mid x_{k+1} = w_k\}.$$

Remark 1 *To ensure that the reformulation to Problem (1) has a strictly convex objective function that is equivalent to that of Problem (3), the objective for x_{k+1} needs to be distributed between x_{k+1} and w_k in the following way:*

$$\alpha_k(x_{k+1} - \bar{x}_{k+1})^\top Q_{k+1}(x_{k+1} - \bar{x}_{k+1})^\top + (1 - \alpha_k)(w_k - \bar{x}_{k+1})^\top Q_{k+1}(w_k - \bar{x}_{k+1})^\top$$

for each k and any $\alpha_k \in (0, 1)$. Together with the coupling constraint $w_k = x_{k+1}$ this ensures that the cost remains unchanged. In this work, we have used $\alpha_k = 0.5$ for all k . The construction of appropriate $H \succ 0$ and h follows immediately.

3 KKT conditions for Problem (2)

We investigate Karush-Kuhn-Tucker (KKT) conditions for Problem (2) and construct an operator K_ξ for finding particular KKT points. The properties and structure of this operator play an important role in showing local optimality and local convergence properties, as well as establishing the computational efficiency of the developed algorithm.

3.1 Generalized, regular \mathcal{E} proximal KKT points

In the context of convex optimization the KKT conditions give rise to necessary and sufficient conditions for global optimality. In the non-convex, non-smooth case, however, they are in general neither necessary nor sufficient, even for local optimality. We first define a notion of KKT points for the problems considered here. We will show that for instances of Problem (2), they give rise to necessary conditions for local optimality. Computing such KKT points is in general intractable. Therefore, we will propose two inner approximations that are more computationally attractive. We will denote KKT points by \dagger , local optima by \circ and global optima by \star .

A point $(z^\dagger, y^\dagger, \lambda^\dagger)$ is called a (generalized) KKT point [30, Theorem 3.34, p. 127] of Problem (2) if it satisfies

$$0 \in \partial\left(\frac{1}{2}z^\top H z + h^\top z + \chi_{\mathcal{E}}(z) + \chi_{\mathcal{Z}}(y)\right)(z^\dagger, y^\dagger) - \{\nabla\langle \lambda^\dagger, z - y \rangle(z^\dagger, y^\dagger)\}, \quad (5a)$$

$$0 = z^\dagger - y^\dagger, \quad (5b)$$

where (5a) is called the *stationarity* condition and (5b) is the *primal feasibility* condition. We can simplify (5), by using $z^\dagger = y^\dagger$, and the following two facts about subdifferentials: (i) the subdifferential $\partial f(x)$ of the sum $f := g + f_0$ of a finite function g and a smooth function f_0 is simply $\partial f(x) = \partial g(x) + \{\nabla f_0(x)\}$, see [31, Exercise 8.8, p. 304]; (ii) the sum of two separable functions $f(x) + g(y)$ has a decoupled subdifferential $\partial f(x) \times \partial f(y)$, see [31, Proposition 10.5, p. 426]. This implies that (5) is equivalent to

$$0 \in \{H z^\dagger + h\} + \mathcal{N}_{\mathcal{E}}(z^\dagger) - \{\lambda^\dagger\}, \quad (6a)$$

$$0 \in \mathcal{N}_{\mathcal{Z}}(y^\dagger) + \{\lambda^\dagger\}, \quad (6b)$$

$$0 = z^\dagger - y^\dagger, \quad (6c)$$

where the regular normal cone of a set \mathcal{C} is denoted by

$$\hat{\mathcal{N}}_{\mathcal{C}}(z) := \left\{ x \in \mathbb{R}^n \mid \limsup_{\substack{u \rightarrow z \\ \mathcal{C}}} \frac{\langle x, u - z \rangle}{\|u - z\|} \right\},$$

and \mathcal{N}_C denotes the (limiting) normal cone, i.e.,

$$\mathcal{N}_C(z) := \limsup_{x \xrightarrow{c} z} \hat{\mathcal{N}}_C(x) = \partial\chi_C(z),$$

as defined in [31, Proposition 6.5, p. 200]. In particular, this implies that $z^\dagger = y^\dagger \in \mathcal{E} \cap \mathcal{Z}$. Since any KKT point $(z^\dagger, y^\dagger, \lambda^\dagger)$ satisfies primal feasibility, $z^\dagger = y^\dagger$, we will use the shorthand notation $(z^\dagger, \lambda^\dagger)$ for KKT points in the remainder of this paper. The KKT conditions (6) give rise to necessary conditions for local optimality as detailed below.

Lemma 1 (Necessary optimality condition) *For every local minimum z° of Problem (2) there exist Lagrange multipliers $\lambda^\circ \in \mathbb{R}^n$ such that (z°, λ°) is a (generalized) KKT point of Problem (2).*

PROOF. Problem (2) satisfies the linear constraint qualification [32, Corollary 4.8, p. 958], which, via [32, Theorem 3.6, p. 950], implies that for every local minimum z° of Problem (2) there exists a $\lambda^\circ \in \mathbb{R}^n$ such that (z°, λ°) is a KKT point of Problem (2). \square

These KKT conditions are difficult to use due to the dependence on the normal cone of \mathcal{Z} , which cannot be evaluated easily [33]. However, we can define two inner approximations that admit practical characterizations, resulting in what we call *regular* and ξ -*proximal* KKT points. These special cases of KKT points can be evaluated more efficiently and have important regularity properties. Furthermore, in Section 4.2, we will show that they provide sufficient (but no longer necessary) conditions for local optimality.

We call a point $(z^\dagger, \lambda^\dagger)$ a *regular* KKT point of Problem (2), if it satisfies

$$0 \in \{Hz^\dagger + h\} + \hat{\mathcal{N}}_{\mathcal{E}}(z^\dagger) - \{\lambda^\dagger\}, \text{ and} \quad (8a)$$

$$0 \in \hat{\mathcal{N}}_{\mathcal{Z}}(z^\dagger) + \{\lambda^\dagger\}. \quad (8b)$$

Note that we have replaced the (limiting) normal cone $\mathcal{N}_{\mathcal{Z}}(z^\dagger)$ with the regular normal cone $\hat{\mathcal{N}}_{\mathcal{Z}}(z^\dagger)$ from (6b). Since $\hat{\mathcal{N}}_{\mathcal{Z}}(z^\dagger) \subseteq \mathcal{N}_{\mathcal{Z}}(z^\dagger)$, according to [31, Proposition 6.5 6(7), p. 200], the set of regular KKT points is an inner approximation of the set of (generalized) KKT points. We remark that for convex problems, i.e., when \mathcal{Z} is convex, we have $\mathcal{N}_{\mathcal{Z}} = \hat{\mathcal{N}}_{\mathcal{Z}}$ and therefore generalized KKT points are also regular.

Given $\xi > 0$, we call a point $(z^\dagger, \lambda^\dagger)$ a ξ -*proximal* KKT point of Problem (2), if it satisfies

$$0 \in \{Hz^\dagger + h\} + \hat{\mathcal{N}}_{\mathcal{E}}(z^\dagger) - \{\lambda^\dagger\}, \text{ and} \quad (9a)$$

$$z^\dagger \in \mathcal{P}_{\mathcal{Z}}(z^\dagger - \frac{1}{\xi}\lambda^\dagger). \quad (9b)$$

Compared to the definition of regular KKT points we have replaced (8b) with a condition on the projection, and we have introduced a positive scaling ξ using $z^\dagger \in \mathcal{P}_{\mathcal{Z}}(z^\dagger - \frac{1}{\xi}\lambda^\dagger) \Rightarrow -\frac{1}{\xi}\lambda^\dagger \in \hat{\mathcal{N}}_{\mathcal{Z}}(z^\dagger)$, which follows from [31, Example 6.16, p. 212]. This directly implies that every ξ -proximal KKT point $(z^\dagger, \lambda^\dagger)$ is also a regular KKT point and therefore (9) is an inner approximation of (8). We will denote the set of all multipliers λ^\dagger that correspond to a given z^\dagger such that $(z^\dagger, \lambda^\dagger)$ is a ξ -proximal KKT point by

$$\mathcal{D}_\xi^\pi(z^\dagger) := \{\lambda^\dagger \mid (z^\dagger, \lambda^\dagger) \text{ satisfy (9)}\}, \quad (10)$$

which, for fixed z^\dagger , is a convex set by virtue of the fact that the proximal normal cone of \mathcal{Z} is a convex cone [31, p. 213].

Evaluating whether a pair (z, λ) is a regular KKT point has an exponential worst-case complexity, because representing $\hat{\mathcal{N}}_{\mathcal{Z}}(z)$ may be combinatorial, and can quickly become intractable. In contrast, evaluating whether a pair (z, λ) is a ξ -proximal KKT point amounts to a projection that can be performed in polynomial-time, as mentioned

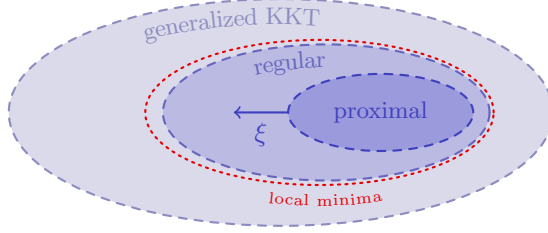


Fig. 1. Conceptual illustration of the relationship between generalized, regular and proximal KKT points (dashed). In particular the sets represent points z for which there exist multipliers λ such that (z, λ) is a generalized, regular or proximal KKT point, as well as the set of local minima (dotted).

in Section 2. Furthermore, for the primal variables z , this inner approximation (9) of (8) can be made tight. This can be seen via the following proposition which relates any regular KKT to a ξ -proximal KKT point. The conceptual relationship between generalized, regular and ξ -proximal KKT points is illustrated in Figure 1.

Proposition 1 Consider Problem (2). Then

- i) for any regular KKT point $(z^\dagger, \lambda^\dagger)$, there exists a $\bar{\xi} > 0$ such that for all $\xi \geq \bar{\xi}$, we have that $(z^\dagger, \lambda^\dagger)$ is a ξ -proximal KKT point.
- ii) Given any $\xi > 0$, and ξ -proximal KKT point $(z^\dagger, \lambda^\dagger)$. $(z^\dagger, \lambda^\dagger)$ is also a regular KKT point.

Problem (2) has only finitely many local minima, due to positive definiteness of H and the polyhedrality of $\mathcal{E} \cap \mathcal{Z}$. This means that, given a $\xi > 0$ large enough, for every regular KKT point $(z^\dagger, \lambda^\dagger)$, there exists a μ^\dagger such that (z^\dagger, μ^\dagger) is a ξ -proximal KKT point.

3.2 Operator for proximal KKT points

The polynomial-time set-membership evaluation of (9) motivates the construction of an operator K_ξ , that has the property that (i) it is cheap to evaluate and (ii) has zeros corresponding to ξ -proximal KKT points of Problem (2). We define a set-valued operator $K_\xi : \mathbb{R}^n \rightrightarrows \mathbb{R}^n$:

$$K_\xi(s) := \{M_\xi s + c_\xi\} - \mathcal{P}_{\mathcal{Z}}(s), \quad (11a)$$

with $\xi > 0$ the proximal scaling, and

$$M_\xi := \xi (\xi R - I)^{-1} R, \quad (11b)$$

$$c_\xi := (\xi R - I)^{-1} (R(h + H\bar{v}) - \bar{v}), \quad (11c)$$

$$R := V(V^\top H V)^{-1} V^\top, \quad (11d)$$

where V and \bar{v} are as defined in (1f). To understand this choice of K_ξ , consider $z := R(\lambda - h - H\bar{v}) + \bar{v}$, which characterizes the unique solution of $0 \in \{Hz + h - \lambda\} + \hat{\mathcal{N}}_{\mathcal{E}}(z)$. After substituting λ with $s := z - \frac{1}{\xi}\lambda$ in the definition of z , we see that z satisfies $0 \in \{Hz + h - \lambda\} + \hat{\mathcal{N}}_{\mathcal{E}}(z)$ if and only if $z = M_\xi s + c_\xi$, which means that $0 \in K_\xi(s)$ is equivalent to $z = M_\xi s + c_\xi \in \mathcal{P}_{\mathcal{Z}}(s)$. Therefore, it is sufficient to find a point s satisfying $0 \in K_\xi(s)$, in order to find a primal point z satisfying the ξ -proximal KKT conditions in (9).

For the operator K_ξ to be defined properly, we need $\xi R - I$ to be invertible. From $R \succeq 0$, it follows that $\xi R - I$ is invertible for all

$$\xi > \frac{1}{\lambda_{\min}^+(R)}, \quad (12a)$$

where $\lambda_{\min}^+(R)$ is the smallest non-zero eigenvalue of R . This can always be achieved via the choice of ξ . Finally, we note that (12a) implies $M_\xi \succeq 0$ and

$$\lambda_{\min}^+(M_\xi) > 1. \quad (12b)$$

In fact, if $Hu \in \text{range } V$ for all $u \in \text{range } V$, as is the case for hybrid MPC Problem (3), it can be shown that $\xi > \lambda_{\max}(H)$ is necessary and sufficient for satisfying both (12a) and (12b). Note that to achieve the theoretical guarantees in Section 4, we will need to impose further restrictions on ξ .

Using the definition of K_ξ in (11a) we can show that points $s^\dagger \in \text{zero } K_\xi$, correspond to ξ -proximal KKT points $(z^\dagger, \lambda^\dagger)$ in the following way

$$z^\dagger := M_\xi s^\dagger + c_\xi, \text{ and} \tag{13a}$$

$$\lambda^\dagger := \xi(z^\dagger - s^\dagger), \tag{13b}$$

where the exact relationship is presented in Lemma 2.

Lemma 2 (Zeros of operator K_ξ) *Given any $\xi > 0$. A point s^\dagger is a zero of K_ξ , i.e., $s^\dagger \in \text{zero } K_\xi$, if and only if the pair $(z^\dagger, \lambda^\dagger)$ constructed through (13) is a ξ -proximal KKT point of Problem (2).*

Notice, that M_ξ is not invertible unless $\mathcal{E} = \mathbb{R}^n$, therefore multiple $s^\dagger \in \text{zero } K_\xi$ can result in the same z^\dagger (but different λ^\dagger). Lemma 2 tells us that given a zero s of K_ξ , it is straightforward to reconstruct a corresponding KKT point, using (13).

4 Method

In this section, we present a method for finding ξ -proximal KKT points of Problem (2) by finding zeros of the operator K_ξ . The basis of this method will be a fixed-point iteration. We have argued that K_ξ can be evaluated efficiently because it only involves matrix-vector multiplications and a small number of projections onto convex polyhedra. This means that every iteration of our method is computationally inexpensive. In addition, we will show that every zero of K_ξ corresponds to a local minimum of Problem (2). Furthermore, we will show that, under some assumptions, our algorithm converges locally to such minima, almost always. By ‘almost always’ we mean that, for any local minimum that has corresponding fixed points, there exist at most a measure-zero subset of fixed points from which the method may not converge.

4.1 Fixed-point algorithm

We first define an operator $T_\xi : \mathbb{R}^n \rightrightarrows \mathbb{R}^n$, that has the zeros of K_ξ as its fixed points:

$$T_\xi(s) := s - WK_\xi(s) \tag{14a}$$

$$= s - W(M_\xi s + c_\xi - \mathcal{P}_Z(s)) \tag{14b}$$

$$= (I - WM_\xi)s - Wc_\xi + W\mathcal{P}_Z(s). \tag{14c}$$

The weighting matrix W , chosen as

$$W := Q \begin{pmatrix} \frac{1}{2}\Lambda^{-1} & 0 \\ 0 & -I \end{pmatrix} Q^\top, \tag{14d}$$

is invertible. $Q \in \mathbb{R}^{n \times n}$ is an orthonormal matrix and $\Lambda \in \mathbb{R}^{n-m \times n-m}$ diagonal, positive definite, such that $M_\xi = Q \text{diag}(\Lambda, 0) Q^\top$ is the eigendecomposition of M_ξ . The invertibility of W ensures that $\text{fix } T_\xi = \text{zero } K_\xi$. In addition, the structure of W will be used to prove local non-expansiveness of the operator T_ξ , see Lemma 5 in Section 4.4. To achieve that, intuitively, W is chosen such that $I - WM_\xi$ and $W\mathcal{P}_Z$ balance each other.

The local non-expansiveness of T_ξ allows us to use the *Krasnoselskij iteration* [34, Theorem 3.2, p. 65] to find fixed points of T_ξ . Given an initial iterate s_0 , the Krasnoselskij iteration is defined as follows:

$$s_{j+1} = (1 - \gamma)s_j + \gamma T_\xi(s_j),$$

with step size $\gamma \in (0, 1)$. The step size γ represents the convex combination between the previous iterate s_j and the ‘update’ $T_\xi(s_j)$. For γ close to zero, we update slowly, whereas for γ close to one, we rely almost fully on $T_\xi(s_j)$.

Applying the definition of T_ξ we obtain Algorithm 1 (see below). Initially, the algorithm checks whether there is a trivial solution z^* , that effectively minimizes the objective $\frac{1}{2}z^\top H z + h^\top z$ on \mathcal{E} . If $z^* \in \mathcal{Z}$, we have found a global optimum and the algorithm terminates. If this is not the case, the Krasnoselskij iteration is employed to compute a fixed point of T_ξ , which corresponds to a local minimum. Each iteration of Algorithm 1 is very simple

and geared towards efficient embedded implementations utilizing automatic code-generation. The most expensive step being the projection onto the non-convex set \mathcal{Z} in step 6. For problems of the form (3), the matrices M_ξ and W are block-banded with bandwidth $\max\{2n_x, n_u\}$, therefore lines 5 and 7 of Algorithm 1 can be evaluated very efficiently and have a computational complexity of $\mathcal{O}(N(n_x + n_u)^2)$. The projection step in line 6 can be evaluated in polynomial time using Algorithm 2, where at most $\sum_{k=1}^N m_k$ small-scale projections $\mathcal{P}_{\mathcal{Z}_{k,i}(\theta)}(s_k)$ onto polyhedra need to be computed. State-of-the-art embedded solvers [35–37] or even explicit solutions [38, 39] can be used for these projections. This enables the automatic generation of efficient, embeddable code that is tailored to a particular (parametric) problem.

Algorithm 1 Low-complexity, iterative algorithm for solving Problem (2)

Require: $s_0 \in \mathbb{R}^n$, $\gamma \in (0, 1)$, $\epsilon_{\text{tol}} > 0$

```

1: if  $z^* := \bar{v} - R(h + H\bar{v}) \in \mathcal{Z}$  then
2:   return  $z^*$ 
3:  $j = 0$ 
4: repeat
5:    $z_{j+1} = M_\xi s_j + c_\xi$ 
6:    $y_{j+1} \in \mathcal{P}_{\mathcal{Z}}(s_j)$ 
7:    $s_{j+1} = s_j - \gamma W(z_{j+1} - y_{j+1})$ 
8:    $j \leftarrow j + 1$ 
9: until  $\|z_{j+1} - y_{j+1}\| \leq \epsilon_{\text{tol}}$ 
10: return  $y_{j+1}$ 

```

▷ Projection, see Alg. 2

Algorithm 2 Projection $\mathcal{P}_{\mathcal{Z}}(s)$

Require: $s = (s_1, \dots, s_N) \in \mathbb{R}^n$, \mathcal{Z}

```

1: for  $k = 1, \dots, N$  do
2:   for  $i = 1, \dots, m_k$  do
3:      $z_{k,i} = \mathcal{P}_{\mathcal{Z}_{k,i}}(s_k)$ 
4:    $z_k \in \arg \min_{i=1, \dots, m_k} \|s_k - z_{k,i}\|$ 
return  $z = (z_1, \dots, z_N)$ 

```

▷ simple

It should be noted that while the simplicity of Algorithm 1 is reminiscent of ADMM, the algorithms have important differences that make it possible to give convergence guarantees in our case. ADMM operates on the primal variables z , y and the Lagrange multipliers λ . In contrast, our method is an iteration on only one variable, namely s , which can be seen as a mixture of primal and dual variables. Furthermore, the iterates z_j and $\lambda_j := \xi(z_{j+1} - s_j)$, always satisfy the first part (9a) of the KKT conditions, which in ADMM is only the case as the algorithm converges.

4.2 Local optimality

Firstly, we will show that any regular KKT point of Problem (2) corresponds to a local minimum of Problem (2). This immediately implies that the fixed points of the operator T_ξ also correspond to local minima. Using distributivity of the Cartesian product over unions, we can transform the representation (1c) of \mathcal{Z} into a representation as the finite union of closed, convex polyhedra $\mathcal{Z}^i \subseteq \mathbb{R}^n$:

$$\mathcal{Z} = \bigcup_{i=1}^I \mathcal{Z}^i, \quad (15)$$

where $I := \prod_{k=1}^N m_k$. For the purpose of this paper, it is only important to notice that (1c) always admits a representation of form (15). Since we now discuss the theoretical properties of our algorithm, the exact construction of the sets \mathcal{Z}^i does not affect the results presented. Although not suited for computational purposes, representation (15) helps to simplify our theoretical considerations. Furthermore, we define the *set of active components* of \mathcal{Z} at a point $z \in \mathcal{Z}$ as $\mathcal{I}_{\mathcal{Z}}(z) := \{i \in \{1, \dots, I\} \mid z \in \mathcal{Z}^i\}$.

To establish this local optimality result, we first show that instead of the regular normal cone $\hat{\mathcal{N}}_{\mathcal{Z}}$ of \mathcal{Z} , we can consider the normal cone of a closed convex set that involves the polar cone $\hat{\mathcal{N}}_{\mathcal{Z}}^*$ defined in [31, Equation 6(14)],

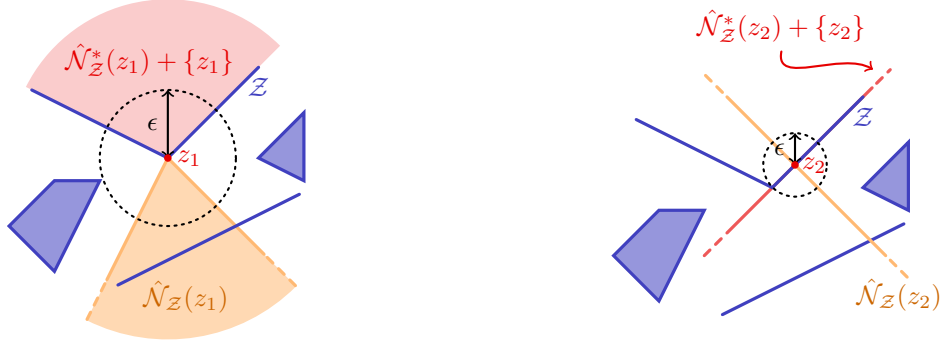


Fig. 2. Two cases of local convexifications $\hat{\mathcal{N}}_{\mathcal{Z}}^*(z) + \{z\}$ of the non-convex set \mathcal{Z} at points z_1 (left) and z_2 (right), as described in Lemma 3.

p. 215] as

$$\hat{\mathcal{N}}_{\mathcal{Z}}^*(z) = \{v \mid \langle v, w \rangle \leq 0, \forall w \in \hat{\mathcal{N}}_{\mathcal{Z}}(z)\}. \quad (16a)$$

From [31, Theorem 6.9, p. 203], we will also use the fact that the normal cone of a closed convex set \mathcal{C} can be expressed as

$$\hat{\mathcal{N}}_{\mathcal{C}}(z) = \{v \mid \langle v, u - z \rangle \leq 0, \forall u \in \mathcal{C}\}. \quad (16b)$$

The following lemma establishes two important properties of the set \mathcal{Z} and its normal cone. These properties will be used in Theorem 1 for proving local optimality. At any point $z \in \mathcal{Z}$, Lemma 3 relates the set \mathcal{Z} to a local convexification $\hat{\mathcal{N}}_{\mathcal{Z}}^*(z) + \{z\}$. This is illustrated in Figure 2.

Lemma 3 (Local convexification of \mathcal{Z}) *For any $z \in \mathcal{Z}$, the set \mathcal{Z} and the closed convex set $\hat{\mathcal{N}}_{\mathcal{Z}}^*(z) + \{z\}$ are related in the following ways:*

i) *There exists an $\bar{\epsilon} > 0$ such that for all $\epsilon \in (0, \bar{\epsilon}]$ the following holds:*

$$\mathcal{Z} \cap \mathcal{B}_{\epsilon}(z) \subseteq \hat{\mathcal{N}}_{\mathcal{Z}}^*(z) + \{z\}. \quad (17a)$$

ii) *Their regular normal cones, evaluated at z , coincide, i.e.,*

$$\hat{\mathcal{N}}_{\mathcal{Z}}(z) = \hat{\mathcal{N}}_{\hat{\mathcal{N}}_{\mathcal{Z}}^*(z) + \{z\}}(z). \quad (17b)$$

We now use Lemma 3 to prove the first key result.

Theorem 1 (Sufficient local optimality condition) *If $(z^\dagger, \lambda^\dagger)$ is a regular KKT point of Problem (2), then z^\dagger is a local minimum of Problem (2).*

PROOF. Let $(z^\dagger, \lambda^\dagger)$ be a regular KKT point of Problem (2). The following problem is a variant of Problem (2), in which the non-convex set \mathcal{Z} is replaced with the local convexification of \mathcal{Z} at $z^\dagger \in \mathcal{Z}$:

$$\min_{z, y} \frac{1}{2} z^\top H z + h^\top z \quad (18a)$$

$$\text{s. t. } (z, y) \in \mathcal{E} \times \left(\hat{\mathcal{N}}_{\mathcal{Z}}^*(z^\dagger) + \{z^\dagger\} \right), \quad (18b)$$

$$z = y. \quad (18c)$$

Problem (18) is strictly convex and its KKT conditions are given as $z = y$ (primal feasibility) and

$$0 \in \{H z + h\} + \hat{\mathcal{N}}_{\mathcal{E}}(z) - \{\lambda\}, \quad (19a)$$

$$0 \in \hat{\mathcal{N}}_{\hat{\mathcal{N}}_{\mathcal{Z}}^*(z^\dagger) + \{z^\dagger\}}(y) + \{\lambda\}. \quad (19b)$$

By Lemma 3(ii), (19b) is equivalent to (8b). Therefore, using $z^\dagger \in \mathcal{Z}$, and the fact that $(z^\dagger, \lambda^\dagger)$ is a regular KKT point, we see that $(z^\dagger, \lambda^\dagger)$ also satisfies conditions (19). This means that $(z^\dagger, \lambda^\dagger)$ is also a regular KKT point of

Problem (18). By strict convexity, implied by $H \succ 0$, it is therefore a (generalized) KKT point of Problem (18) and thus, it is primal-dual optimal for Problem (18). Furthermore, using Lemma 3(i), we know that there exists an $\epsilon > 0$ such that $z^\dagger \in \mathcal{Z} \cap \mathcal{B}_\epsilon(z^\dagger) \subseteq \hat{\mathcal{N}}_{\mathcal{Z}}^*(z^\dagger) + \{z^\dagger\}$, therefore, the pair $y = z = z^\dagger$ is also optimal for the non-convex program

$$\min_{z,y} \frac{1}{2} z^\top H z + h^\top z \tag{20a}$$

$$\text{s. t. } (z, y) \in \mathcal{E} \times (\mathcal{Z} \cap \mathcal{B}_\epsilon(z^\dagger)) , \tag{20b}$$

$$z = y . \tag{20c}$$

Notice that Problem (20) is a local instance of Problem (1), and therefore of Problem (2), where the feasible region is intersected with $\mathcal{B}_\epsilon(z^\dagger)$. This implies that z^\dagger is locally optimal for Problem (2). \square

Theorem 1 allows us to reconstruct a local minimum z° from any zero $s^\circ \in \text{zero } K_\xi$, and therefore from any fixed point of T_ξ , using (13a).

4.3 Existence

We now consider the existence of fixed points of T_ξ . In Proposition 1 we have seen, that for any regular KKT point, by choosing the proximal scaling ξ large enough, we can ensure the existence of a ξ -proximal KKT point. This implies that, if there exists a regular KKT point, we can ensure that the operator T_ξ has at least one fixed point, which is a precursor to convergence, and the second key result.

Theorem 2 (Existence of fixed points of T_ξ) *If there exists a regular KKT point $(z^\dagger, \lambda^\dagger)$ of Problem (2), then there exists a $\bar{\xi} > 0$ such that T_ξ has at least one fixed point for any $\xi \geq \bar{\xi}$.*

PROOF. Given a regular KKT point $(z^\dagger, \lambda^\dagger)$ of Problem (2), and using Proposition 1(i), we know that there exists a $\bar{\xi} > 0$ such that for any $\xi \geq \bar{\xi}$ we have that $(z^\dagger, \lambda^\dagger)$ is a ξ -proximal KKT point. Therefore, by Lemma 2, $s^\dagger := z^\dagger - \frac{1}{\xi} \lambda^\dagger \in \text{zero } K_\xi$ and thus s^\dagger is a fixed point of T_ξ . \square

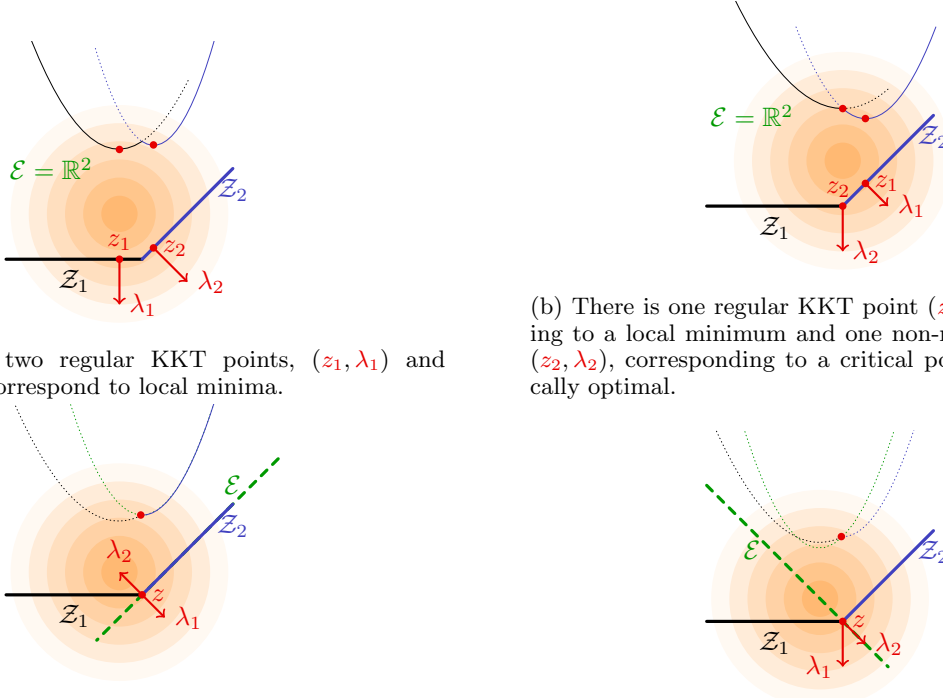
In Figure 3 we illustrate three cases for the existence and nature of KKT points, and also give an example where the operator T_ξ fails to have any fixed points. Figures 3a–3c are cases where the proximal scaling ξ can be chosen such that fixed points of T_ξ exists. Figures 3a and 3b illustrate common cases. On the other hand Figure 3c depicts a more rare case where both regular as well as non-regular multipliers, i.e., multipliers that are generalized, but not regular, exist for the same optimum. In all of these three cases existence is ensured for any $\xi > 0$ and we may find local minima using the proposed method. Finally, Figure 3d illustrates a degenerate case where the feasible set is a singleton and none of the KKT points corresponding to this point are regular. In this case operator T_ξ would not have a fixed point for any $\xi > 0$, even though a (generalized) KKT point exists.

4.4 Local convergence

In this section, we give a proof of local convergence for the method presented in this paper. This proof is based on local properties of the projection operator $\mathcal{P}_{\mathcal{Z}}$. We will show that the projection operator is single-valued, continuous and firmly non-expansive in a neighborhood around (almost) every fixed point $s \in \text{fix } T_\xi$. This translates to the local non-expansiveness of T_ξ , which, in turn, enables the convergence of the Krasnoselskij iteration.

We say that a fixed point s° *corresponds* to a local minimum z° , if the ξ -proximal KKT point (z°, λ°) can be constructed from s° through (13). Note that, as shown in Lemma 2 and Theorem 1, any fixed point of T_ξ can be used to reconstruct a local minimum. We denote the set of fixed points corresponding to z° by

$$\begin{aligned} \text{fix } T_\xi | z^\circ &:= \{s \mid \xi(z^\circ - s) \in \mathcal{D}_\xi(z^\circ)\} \\ &= \{s \mid 0 \in \{H z^\circ + h - \xi(z^\circ - s)\} + \hat{\mathcal{N}}_{\mathcal{E}}(s^\circ), z^\circ \in \mathcal{P}_{\mathcal{Z}}(s)\} , \end{aligned}$$



(a) There are two regular KKT points, (z_1, λ_1) and (z_2, λ_2) . Both correspond to local minima.

(b) There is one regular KKT point (z_1, λ_1) , corresponding to a local minimum and one non-regular KKT point (z_2, λ_2) , corresponding to a critical point that is not locally optimal.

(c) There is one non-regular KKT point (z, λ_1) corresponding to the unique global minimum. However (z, λ_2) is a regular KKT point that corresponds to the same global minimum.

(d) There are only two KKT points (z, λ_1) and (z, λ_2) corresponding to the unique global minimum, both are non-regular.

Fig. 3. Illustration of KKT points of the problem $\min_{z,y \in \mathcal{E} \times (\mathcal{Z}_1 \cup \mathcal{Z}_2)} \frac{1}{2}z^\top z + h^\top z$ s. t. $z = y$. The **level curves** of the objective are given and the objective value evaluated on \mathcal{Z}_1 , \mathcal{Z}_2 and \mathcal{E} is shown in the respective colors. It is solid where feasible, and dotted where infeasible. KKT points represent global or local minima, and critical points.

where in the second step we have used (10) and (9), respectively. The sets $\text{fix } T_\xi | z^\circ$ are closed, convex, and have the property that, roughly speaking, they can only grow with growing ξ . An implication of this is detailed in Proposition 2.

Proposition 2 *There exists a $\bar{\xi} > 0$ such that for any local optimum z° , $\text{fix } T_\xi | z^\circ$ is either*

- i) empty, for all $\xi \geq \bar{\xi}$, or*
- ii) a singleton set, for all $\xi \geq \bar{\xi}$, or*
- iii) it contains more than one element, for all $\xi \geq \bar{\xi}$.*

We make the following assumptions:

(A1) Problem (2) has at least one regular KKT point.

(A2) There exists a $\bar{\xi} > 0$ such that

(i) $\bar{\xi} > \lambda_{\min}^+(R)^{-1}$, i.e., (12a),

(ii) $\bar{\xi}$ satisfies Proposition 2, and

(iii) for any local optimum z° , and any $\xi \geq \bar{\xi}$, for which $\text{fix } T_\xi | z^\circ \neq \emptyset$, there exists a fixed point $s^\circ \in \text{fix } T_\xi | z^\circ$ that satisfies $s^\circ \in \text{relint } \hat{\mathcal{N}}_{\mathcal{Z}}(z^\circ) + \{z^\circ\}$.

(A3) The structure of set \mathcal{Z} is such that, for any $z \in \mathcal{Z}$, either $\hat{\mathcal{N}}_{\mathcal{Z}}(z) = \{0\}$, or there exists an $\epsilon > 0$ such that for all $w \in \hat{\mathcal{N}}_{\mathcal{Z}}(z)^\perp \cap \mathcal{B}_\epsilon$, we have $z + w \in \mathcal{Z}$.

Assumption (A1) ensures the existence of regular KKT points, avoiding degenerate cases such as the one depicted in Figure 3d. Together with the choice of $\xi \geq \bar{\xi}$ from Assumption (A2)(ii), it furthermore implies the existence of fixed points of T_ξ . In addition, the choice of $\xi \geq \bar{\xi}$ in Assumption (A2)(i) ensures that $\lambda_{\min}^+(M_\xi) > 1$ holds. Assumption (A2)(iii) can be understood as a *non-degeneracy* condition on the multipliers because $s^\circ \in \text{relint } \hat{\mathcal{N}}_{\mathcal{Z}}(z^\circ) + \{z^\circ\}$ is equivalent to $-\lambda^\circ \in \text{relint } \hat{\mathcal{N}}_{\mathcal{Z}}(z^\circ)$, with $\lambda^\circ := \xi(z^\circ - s^\circ)$ being the multiplier corresponding to z° , i.e., there exists

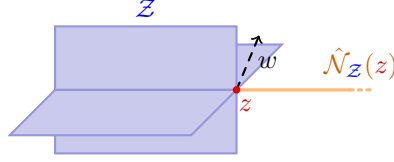


Fig. 4. A set \mathcal{Z} where (A3) is violated at point z . We see that $w \in \hat{\mathcal{N}}_{\mathcal{Z}}(z)$, but $z + \epsilon w \notin \mathcal{Z}$ for all $\epsilon > 0$.

multipliers in the relative interior of $\hat{\mathcal{N}}_{\mathcal{Z}}(z^\circ)$. Finally, (A3) is an assumption on the geometry of \mathcal{Z} . It is satisfied by the sets in Figure 2 and Figure 3, whereas Figure 4 illustrates a simple counter-example in three dimensions. It is not clear whether (A3) holds for all problems of the form of Problem (3). However, since it is a property of the geometry of \mathcal{Z} , it is possible to check numerically whether (A3) holds for a given (possibly parametric) set \mathcal{Z} . In Appendix B, we provide Algorithm 3 and Lemma B.1 to check whether this assumption holds, and apply it to the numerical examples in Section 5.

In Algorithm 1, we apply the Krasnoselskij iteration to the operator T_ξ . This iteration is known to converge when the operator is non-expansive. When \mathcal{Z} is convex, the projection operator $\mathcal{P}_{\mathcal{Z}}$ has a stronger condition: firm non-expansiveness. This stronger condition allows to show the non-expansiveness of T_ξ and leads to global convergence of the Krasnoselskij iteration applied to T_ξ . To show *local* convergence for the non-convex case, we only need T_ξ to be non-expansive in a neighborhood around fixed points. Then, if we start in that neighborhood, we will converge via the same argument. This is detailed in Theorem 3. The local non-expansiveness of T_ξ can, similarly to the convex case, be shown via the local firm non-expansiveness of the projection operator $\mathcal{P}_{\mathcal{Z}}$. Using Assumptions (A1)–(A3), in Lemma 4 we show that, in a neighborhood around almost all fixed points, the projection $\mathcal{P}_{\mathcal{Z}}$ behaves like a projection onto a convex set. Therefore, it is locally firmly non-expansive, single-valued and continuous [40, Proposition 4.8, p. 61]. Then, in Lemma 5, we use the local firm non-expansiveness of the projection operator, together with the particular construction of the operator T_ξ , to show that T_ξ is non-expansive, single-valued and continuous in a neighborhood around almost all fixed points. It is known that, for a non-expansive operator, the Krasnoselskij iteration converges in the limit. Therefore, this guarantees the *local* convergence of Algorithm 1 to a local minimum, almost always.

Lemma 4 *Let Assumptions (A1)–(A3) hold. For any $\xi > \bar{\xi}$, and any local minimum z° to Problem (2) with $z^\circ \notin \text{fix } T_\xi$ and $\text{fix } T_\xi|_{z^\circ} \neq \emptyset$; we have that for all fixed points $s^\circ \in \text{fix } T_\xi|_{z^\circ}$, except a measure-zero subset, there exists an $\epsilon > 0$ such that the projection $\mathcal{P}_{\mathcal{Z}}$ is single-valued, continuous and firmly non-expansive on $\mathcal{B}_\epsilon(s^\circ)$.*

Lemma 5 *Let $\xi > 0$ and given any fixed point $s^\circ \in \text{fix } T_\xi$ such that there exists an $\epsilon > 0$, where the projection $\mathcal{P}_{\mathcal{Z}}$ is single-valued, continuous and firmly non-expansive on $\mathcal{B}_\epsilon(s^\circ)$. Then the operator T_ξ is also single-valued, continuous and non-expansive on $\mathcal{B}_\epsilon(s^\circ)$.*

Theorem 3 *Let Assumptions (A1)–(A3) hold. For any $\xi > \bar{\xi}$, and an initial iterate s_0 sufficiently close to a fixed point of T_ξ , Algorithm 1 converges almost always to a fixed point $s^\circ \in \text{fix } T_\xi$. When it converges, the iterates z_j and y_j converge to each other and to a local minimum of Problem (2).*

PROOF. Given Assumption (A2), let $\xi > \bar{\xi}$. Together with Assumption (A1), this implies the existence of fixed points of T_ξ , i.e., $\text{fix } T_\xi \neq \emptyset$. We first consider the case where there exists a fixed point $s^\circ \in \text{fix } T_\xi$ with corresponding local minimum z° such that $s^\circ = z^\circ$. This is the “unconstrained” case, where $(z^\circ, 0)$ is a KKT point of Problem (2). Therefore

$$\begin{aligned} M_\xi z^\circ + c_\xi &\in \mathcal{P}_{\mathcal{Z}}(z^\circ) = \{z^\circ\} \\ \Leftrightarrow z^\circ &= (I - M_\xi)^{-1} c_\xi \\ &= \bar{v} - R(h + H\bar{v}), \end{aligned}$$

with $I - M_\xi$ invertible due to (A2) and (12b). This condition is checked in step 1 of Algorithm 1, if it holds the algorithm terminates and returns z° , a global minimum. If there is no $s^\circ \in \text{fix } T_\xi$ such that the corresponding local minimum z° satisfies $s^\circ = z^\circ$, we can apply Lemma 4. Lemma 4 says that for any local minimum z° , such that $\text{fix } T_\xi|_{z^\circ} \neq \emptyset$, we know ξ can be chosen large enough such that for all $s^\circ \in \text{fix } T_\xi|_{z^\circ}$, except a measure-zero subset, there exists an $\epsilon > 0$ such that the projection $\mathcal{P}_{\mathcal{Z}}$ is single-valued, continuous and firmly-nonexpansive on $\mathcal{B}_\epsilon(s^\circ)$. We now consider any such s° . Using Lemma 5, this in particular means that T_ξ is non-expansive on $\mathcal{B}_\epsilon(s^\circ)$.

Assuming the initial iterate is close enough, i.e., $s_0 \in \mathcal{B}_\epsilon(s^\circ)$, then by the non-expansiveness of T_ξ we know that the iterates will satisfy $s_j \in \mathcal{B}_\epsilon(s^\circ)$ for all $j \geq 0$. The Krasnoselskij iteration applied to T_ξ , in line 7 of Algorithm 1, will converge to a fixed point of T_ξ for any choice of step-size parameter $\gamma \in (0, 1)$ [34, Theorem 3.2, p. 65]. From this, the single-valuedness, and the continuity of T_ξ , convergence to “consensus” with $\lim_{j \rightarrow \infty} \|z_j - y_j\| = 0$, immediately follows. By Theorem 1, this gives convergence of z_j and y_j to a local minimum of Problem (2). \square

Theorem 3 may require ξ to be large, in order to guarantee convergence. We remark, that a lower bound $\bar{\xi}$, of ξ , satisfying Assumption (A2) may be hard to compute. However, in practice, good results can be obtained for “small” values of ξ . In addition, if the algorithm fails to converge, the theoretical results, through the lower bound $\bar{\xi}$, indicate that choosing a larger value of ξ may improve the convergence behavior. This is verified experimentally in Section 5.3, where we examine the effects of the value of ξ .

Remark 2 (Convex case) *If the set \mathcal{Z} is closed and convex, then the only necessary assumption is that ξ satisfies (12a). In this case the global optimum of Problem (2) corresponds to the unique fixed point of T_ξ and Algorithm 1 converges globally due to strict convexity and the fact that the projection $\mathcal{P}_{\mathcal{Z}}$ is single-valued, continuous and firmly non-expansive everywhere.*

5 Numerical results

In this section, we present numerical results for two MPC examples: (i) a simple example to illustrate the concept, and (ii) a complex one to showcase how the proposed method can be used for realistic problems. We compare our method with a classical MIP reformulation [9] solved using three different commercial MIQP solvers: CPLEX, Gurobi and MOSEK. While we use YALMIP [41] to model the optimization problem, the big-M reformulation is done manually. The reported timings are obtained on an Intel Core i7 processor using a single core running at 2.8 GHz. Efficient C-code for the proposed method was generated automatically integrating the code generated for the individual convex projections using MPT3 [38]. The resulting binaries are 75 kB for Example 5.1, and 550 kB for Example 5.2. In contrast, the executables for CPLEX, Gurobi and MOSEK are in the range of 10 – 20 MB. No warm-starting is used in any example. We also consider the closed-loop behavior, where for every time step a MPC problem with different parameters is solved. These changing parameters are the initial state for Example 5.1, and for Example 5.2 additionally a time-varying reference. The problems are solved in a receding-horizon fashion, where, for each time step, only the first input u_1 is applied to the dynamical system. Then, a new problem with the updated initial state (and reference) is solved for the next time step.

5.1 2-region example

We consider a simple example taken from [9, Example 4.1, p. 415], which consists of a hybrid MPC problem with two states, one input and PWA dynamics defined over two regions:

$$x_{k+1} = \begin{cases} A_1 x_k + B u_k & \text{if } x_{k,1} \geq 0 \\ A_2 x_k + B u_k & \text{if } x_{k,1} \leq 0 \end{cases}, \\ u_k \in [-1, 1].$$

with

$$A_1 = \frac{2}{5} \begin{pmatrix} 1 & -\sqrt{3} \\ \sqrt{3} & 1 \end{pmatrix}, A_2 = \frac{2}{5} \begin{pmatrix} 1 & \sqrt{3} \\ -\sqrt{3} & 1 \end{pmatrix}, B = \begin{pmatrix} 0 \\ 1 \end{pmatrix},$$

and a quadratic regulation objective

$$\sum_{k=1}^N \|x_{k+1}\|^2 + \|u_k\|^2.$$

In this case Assumption (A3) holds and can be verified analytically, using Algorithm 3 in Appendix B. We fix $\xi = 210$, $\gamma = 0.5$ and a consensus tolerance of $\epsilon_{\text{tol}} = 0.001$, and compare our method to CPLEX, Gurobi and MOSEK for different control horizons N . A time limit of $t_{\text{max}} = 1800$ s (30 minutes) is imposed for all solvers. The convergence of our method is illustrated, for $N = 40$, in Figure 5a, which shows a decreasing consensus violation $\|z_j - y_j\|$ for

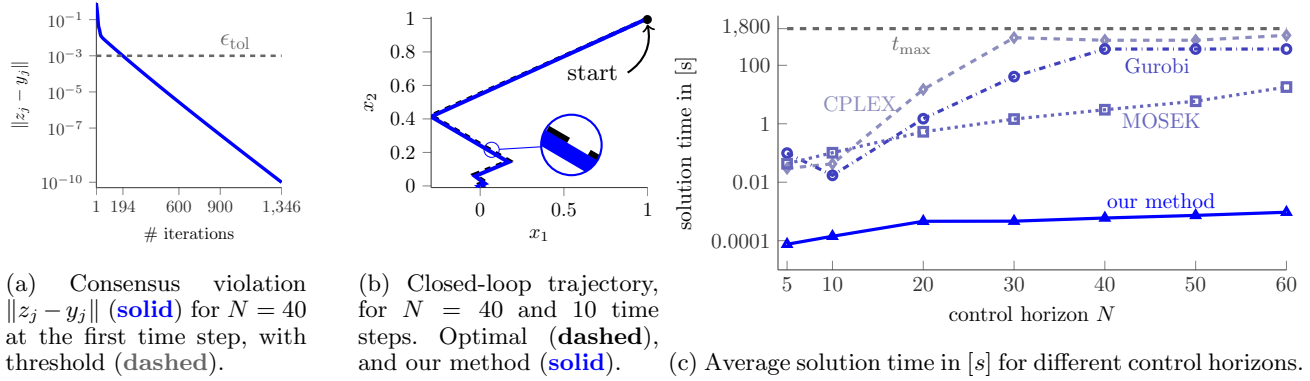


Fig. 5. Comparison of Example 5.1 with $\xi = 210$, $\gamma = 0$ and $\epsilon_{\text{tol}} = 10^{-3}$. The initial state is $x_1 = x_2 = 1$. Our method (solid, \triangle) and a MIP reformulation solved using CPLEX (dashed, \diamond), Gurobi (dash-dotted, \circ) and MOSEK (dotted, \square).

the problem solved at the first time step. The method also converges for all successive time steps (and horizons N), with similar convergence characteristics, which leads to a stable closed-loop trajectory, illustrated in Figure 5b. The trajectory is almost indistinguishable from the optimum (dashed), obtained using a MIP reformulation. The computational advantage of our method is underlined by Figure 5c, where the average runtime for different control horizons N is shown. It shows that our method is several orders of magnitude faster than the considered commercial solvers, and sees only a linear increase in computation time. In contrast, the computation time of CPLEX, Gurobi and MOSEK increases exponentially, with increasing N . As a result, for $N \geq 30$, CPLEX and Gurobi frequently do not terminate before the time limit.

5.2 Racecar example

Mechanical systems are often subject to non-linear friction. We consider an example with a PWA model of the friction forces acting on the tires of a miniature 1:43 RC race car [42]. In [43, p. 108ff] a PWA description based on a bicycle model was developed. The forward velocity v_x of the car is assumed to be fixed to 2 m/s . The state $x = (v_y, \omega)$ of the system consists of the lateral velocity v_y and the turning rate ω . The steering angle δ is the only input to the system. The continuous-time dynamics are described by

$$\begin{aligned} \dot{v}_y &= \frac{1}{m}(F_{f,y}(v_y, \omega, \delta) + F_{r,y}(v_y, \omega) - mv_x\omega), \\ \dot{\omega} &= \frac{1}{I_Z}(l_f F_{f,y}(v_y, \omega, \delta) - l_r F_{r,y}(v_y, \omega)), \end{aligned}$$

where m, I_Z, l_f, l_r are known model parameters and $F_{f,y}, F_{r,y}$ are the non-linear lateral friction forces acting on the front and rear tires of the vehicle, respectively. The friction forces are given as PWA functions with 5 pieces each, leading to a total of 5^2 possible regions, of which 19 are non-empty. With 19 regions this problem is considerably more complex than Example 5.1. The dynamics are discretized with a sampling time of $T_s = 20 \text{ ms}$. Additionally state and input constraints are imposed as follows:

$$\begin{aligned} v_y &\in [-1 \text{ m/s}, 1 \text{ m/s}], & \omega &\in [-8 \text{ rad/s}, 8 \text{ rad/s}], \\ \delta &\in [-23^\circ, 23^\circ]. \end{aligned} \tag{23}$$

The objective is to track a state \bar{x} and input $\bar{\delta}$ reference trajectory that will produce a S-shaped motion of the race car. The chosen objective function is

$$\sum_{k=1}^N (x_{k+1} - \bar{x}_{k+1})^\top Q (x_{k+1} - \bar{x}_{k+1}) + (\delta_k - \bar{\delta}_k)^\top R (\delta_k - \bar{\delta}_k),$$

where

$$Q = \begin{pmatrix} 1 & 0 \\ 0 & 10 \end{pmatrix}, \quad R = 1.$$

As in the previous example, Assumption (A3) is verified numerically, using Algorithm 3. The resulting MPC

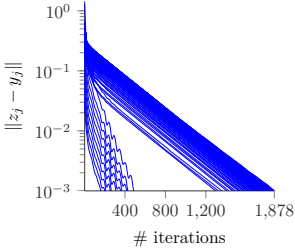


Fig. 6. Consensus violations $\|z_j - y_j\|$ for $N = 20$ and time steps 1 to 150, illustrating convergence.

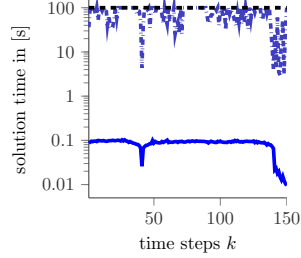


Fig. 7. Solution time in [s] for $N = 20$ with time limit (**dashed**). Our method (**solid**) and Gurobi (**dash-dotted**).

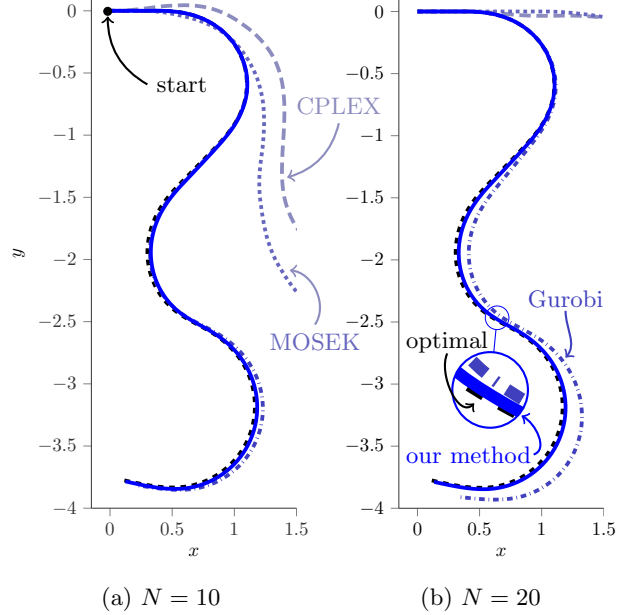


Fig. 8. Closed-loop position trajectory with initial condition $x = y = \varphi = 0$. Our method (**solid**), CPLEX (**dashed**), Gurobi (**dash-dotted**), MOSEK (**dotted**) and optimal (**dashed**).

problems are solved for a prediction horizon of $N = 10$ ($\xi = 290$) and $N = 20$ ($\xi = 400$). In both cases $\gamma = 0.5$ and a consensus tolerance of $\epsilon_{\text{tol}} = 0.001$ is used. We compare the method to the MIP reformulation solved using CPLEX, Gurobi and MOSEK, where a time limit of 15s for $N = 10$, and 100s for $N = 20$ is imposed. Both time limits are significantly above the computation time achieved by our algorithm, which on average requires 0.03s for $N = 10$, and 0.086s for $N = 20$, as reported in Figure 7. Gurobi has an average runtime of 76s for $N = 20$ often reaching the time limit, while CPLEX and MOSEK reach the time limit for every time step. In Figure 6, we show that the method converges in less than 1878 iterations for each of the 150 problems, solved in the closed-loop simulation.

We compare the closed-loop trajectory of the PWA dynamics generated by our method over 150 steps, with the trajectories generated using MIP solvers CPLEX, Gurobi and MOSEK, as well as the optimal trajectory. The initial state is $v_y = \omega = 0$. Notice, that the dynamics of the system are with respect to the lateral and angular velocities, v_y and ω , with a fixed forward velocity $v_x = 2 \text{ m/s}$. It is more intuitive to compare the position of the car, rather than the velocities. Therefore, we use the following *position* dynamics in order to transform the velocities into positions, via integration.

$$\begin{aligned}\dot{x} &= v_x \cos(\varphi) - v_y \sin(\varphi), \\ \dot{y} &= v_x \sin(\varphi) + v_y \cos(\varphi), \\ \dot{\varphi} &= \omega,\end{aligned}$$

The position trajectories of the car are presented in Figure 8. The optimal trajectory is depicted by the **dashed** line, solved using Gurobi without a time limit. Our method (**solid**) significantly outperforms the commercial MIQP solvers in terms of solution quality, coming very close to the optimal trajectory, and in terms of computational performance, requiring 250 – 1000 times less time than the commercial solvers. In particular, for $N = 20$, CPLEX and MOSEK do not manage to return a satisfactory solution within the prescribed time limit of 100s, resulting in especially suboptimal trajectories. Also Gurobi yields a visibly suboptimal trajectory. This illustrates that our method is not only significantly faster, but can also yield superior performance, when there is a time limit for returning a solution. This is of particular importance in a real-time control context.

To illustrate the difference in performance between our method and the commercial MIP solvers, in Table 1, we report the loss of optimality in terms of the percentage gap from the optimal for both $N = 10$ and $N = 20$. Our method has a closed-loop suboptimality of a few percent, whereas the commercial solvers have a dramatic loss of

Solver	$N = 10$		$N = 20$	
	p	$\frac{p-p^*}{p^*}$	p	$\frac{p-p^*}{p^*}$
Our method	5.3	0.5%	5.3	3.2%
Gurobi	26	402%	140	2619%
CPLEX	2022	38398%	5390	104288%
MOSEK	5241	99684%	5945	115030%

Table 1

Suboptimality of the closed-loop simulation for $N = 10$ and $N = 20$, with time limit of 15s and 100s, respectively. The cumulative closed-loop cost of each method is denoted by p , and p^* is the cost obtained with globally optimal solutions.

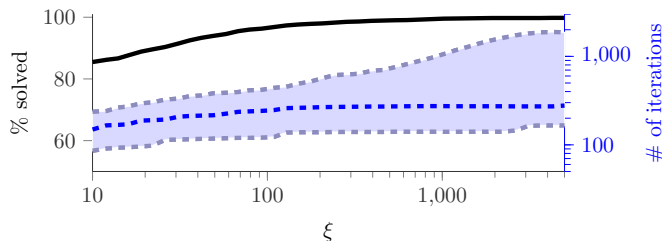


Fig. 9. Illustration of dependence on proximal scaling ξ . Percentage of problems solved (**solid**, left axis) and number of iterations needed to reach 10^{-3} consensus violation (right axis) for the solved problems, median (**dashed**), 5-th and 95-th percentile (**dashed**).

performance due to the imposed time limit. The benchmark cost p^* is computed using Gurobi, warmstarted with our method to achieve practical runtimes. With warmstarting each of the 150 problems can be solved within at most 30 min. Without warmstarting, Gurobi is, in some cases, not able to terminate after 3 hours, with a relative optimality gap of 0.85% still remaining.

5.3 Effect of proximal scaling

In order to better understand the choice of the proximal scaling ξ , we generate 2000 random instances of Example 5.2, with different initial conditions (v_y, ω) satisfying (23), and solve the MPC problem with a horizon of $N = 10$. Of these 2000 problems, 51 were determined to be infeasible using Gurobi, the remaining problems are solved using our method for 40 different values of ξ . Figure 9 demonstrates the relationship between ξ and (i) the relationship and the number of instance that is solved (black), and (ii) the number of iterations needed for the algorithm to converge. We see that for larger ξ more problems are solved, with only 4 (0.2%) unsolved problems remaining for $\xi = 5000$. Furthermore, the number of iterations needed to reach a consensus threshold of 0.001 (right axis) grows only modestly with larger ξ . We note that, in all instances, the constraint violations (mean ≈ 0.001 , standard deviation ≈ 0.0004) and relative suboptimality (mean 0.5 – 1.6%, standard deviation 0.8% – 2.8%) do not change significantly. These findings are consistent with our expectations from the theory, i.e., that larger ξ usually lead to more problems solved but at the expense of slower convergence.

Acknowledgements

The authors would like to thank Sergio Grammatico for helpful discussions.

A Auxiliary propositions & proofs

To prove Proposition 1, we first elaborate on the structure of the regular normal cone of \mathcal{Z} , where the representation (15) is used. Proposition A.1 states, that the regular normal cone of \mathcal{Z} at z can be written as the finite intersection of the normal cones of its convex polyhedral parts \mathcal{Z}^i , where only the sets \mathcal{Z}^i that contain z (i.e. the active components of \mathcal{Z} at z) need to be considered.

Proposition A.1 (Regular normal cone) *The regular normal cone $\hat{\mathcal{N}}_{\mathcal{Z}}$ of \mathcal{Z} evaluated at $z \in \mathcal{Z}$ is given by*

$$\hat{\mathcal{N}}_{\mathcal{Z}}(z) = \bigcap_{i \in \mathcal{I}_{\mathcal{Z}}(z)} \hat{\mathcal{N}}_{\mathcal{Z}^i}(z).$$

PROOF. In [33, p. 59f] it is shown how to represent the normal cone of a finite union of polyhedra in terms of the normal cones of its components. Considering only the regular normal cone and applying this to \mathcal{Z} gives the result. \square

Proof of Proposition 1 We consider the two statements separately.

i) By definition, a regular KKT point (z, λ) satisfies $-\lambda \in \hat{\mathcal{N}}_{\mathcal{Z}}(z)$. We then have by Proposition A.1

$$-\lambda \in \hat{\mathcal{N}}_{\mathcal{Z}}(z) \Rightarrow -\lambda \in \bigcap_{i \in \mathcal{I}_{\mathcal{Z}}(z)} \hat{\mathcal{N}}_{\mathcal{Z}^i}(z).$$

For any $\xi > 0$ this is equivalent to

$$\begin{aligned} \text{(i)} \Leftrightarrow & -\frac{1}{\xi}\lambda \in \hat{\mathcal{N}}_{\mathcal{Z}^i}(z) && \forall i \in \mathcal{I}_{\mathcal{Z}}(z) \\ \Leftrightarrow & z \in \mathcal{P}_{\mathcal{Z}^i}(z - \frac{1}{\xi}\lambda) && \forall i \in \mathcal{I}_{\mathcal{Z}}(z), \end{aligned} \quad (\text{A.1})$$

where (A.1) follows from the convexity of \mathcal{Z}^i and the relationship between the projection $\mathcal{P}_{\mathcal{Z}^i}$ and the normal cone $\hat{\mathcal{N}}_{\mathcal{Z}^i}$, described in [31, p. 212f]. We know by construction that for any $\epsilon > 0$ small enough, we have that $\mathcal{Z} \cap \mathcal{B}_{\epsilon}(z) = \bigcap_{i \in \mathcal{I}_{\mathcal{Z}}(z)} \mathcal{Z}^i \cap \mathcal{B}_{\epsilon}(z)$ and thus

$$(\text{A.1}) \Rightarrow z \in \mathcal{P}_{\mathcal{Z} \cap \mathcal{B}_{\epsilon}(z)}(z - \frac{1}{\xi}\lambda).$$

We now consider $\bar{\xi} = \frac{2}{\epsilon}\|\lambda\|$. For any $\xi \geq \bar{\xi}$ we have $\|(z - \frac{1}{\xi}\lambda) - z\| = \frac{1}{\xi}\|\lambda\| \leq \frac{\epsilon}{2}$ and therefore for all $x \in \mathcal{Z}$ with $\|z - x\| > \epsilon$ we have $\|(z - \frac{1}{\xi}\lambda) - x\| > \frac{\epsilon}{2}$. Together with $z \in \mathcal{P}_{\mathcal{Z} \cap \mathcal{B}_{\epsilon}(z)}(z - \frac{1}{\xi}\lambda)$, this implies that $z \in \mathcal{P}_{\mathcal{Z}}(z - \frac{1}{\xi}\lambda)$ for all $\xi \geq \bar{\xi} = \frac{2}{\epsilon}\|\lambda\|$, which implies that (z, λ) is a ξ -proximal KKT point.

ii) Given any $\xi > 0$, and any ξ -proximal KKT point (z, λ) . By definition, it satisfies $z \in \mathcal{P}_{\mathcal{Z}}(z - \frac{1}{\xi}\lambda)$, which implies $-\frac{1}{\xi}\lambda \in \hat{\mathcal{N}}_{\mathcal{Z}}(z)$ via [31, Example 6.16, p. 212]. This is equivalent to $-\lambda \in \hat{\mathcal{N}}_{\mathcal{Z}}(z)$, which directly implies that (z, λ) is a regular KKT point. \square

Proof of Lemma 2 Given any $\xi > 0$, and any $s^\dagger \in \text{zero } K_\xi$, we know that by definition $0 \in \{M_\xi s^\dagger + c_\xi\} - \mathcal{P}_{\mathcal{Z}}(s^\dagger)$, and thereby $z^\dagger := M_\xi s^\dagger + c_\xi \in \mathcal{P}_{\mathcal{Z}}(s^\dagger)$. We define $\lambda^\dagger := \xi(z^\dagger - s^\dagger)$ and thus we see that

$$z^\dagger \in \mathcal{P}_{\mathcal{Z}}(z^\dagger - \frac{1}{\xi}\lambda^\dagger) \Leftrightarrow (9b) \text{ holds.}$$

Furthermore, we have that $z^\dagger = M_\xi(z^\dagger - \frac{1}{\xi}\lambda^\dagger) + c_\xi$, which, using (11b)–(11d), is equivalent to

$$z^\dagger = R(\lambda^\dagger - h - H\bar{v}) + \bar{v}. \quad (\text{A.2})$$

By strict convexity, we have that z^\dagger , as in (A.2), is the unique solution to

$$\begin{aligned} 0 & \in \partial_z(\frac{1}{2}z^\top H z + h^\top z - \lambda^{\dagger\top} z + \chi_{\mathcal{E}}(z))(z^\dagger) \\ \Leftrightarrow 0 & \in \{H z^\dagger + h - \lambda^\dagger\} + \hat{\mathcal{N}}_{\mathcal{E}}(z^\dagger) \\ \Leftrightarrow & (9a) \text{ holds} \end{aligned}$$

Therefore $(z^\dagger, \lambda^\dagger)$ is a ξ -proximal KKT point if and only if $s^\dagger = z^\dagger - \frac{1}{\xi} \lambda^\dagger \in \text{zero } K_\xi$. \square

Proof of Lemma 3 We prove the two parts individually.

i) Take any $\bar{z} \in \mathcal{Z}$ and any $z \in \mathcal{Z} \cap \mathcal{B}_\epsilon(\bar{z})$. Then using the definition (16a) of the polar cone we have that $z \in \hat{\mathcal{N}}_{\mathcal{Z}}^*(\bar{z}) + \{\bar{z}\}$ if and only if

$$\langle z - \bar{z}, v \rangle \leq 0, \quad \forall v \in \hat{\mathcal{N}}_{\mathcal{Z}}(\bar{z}),$$

We assume for the sake of contradiction that for all $\bar{\epsilon} > 0$ there exists a $v \in \hat{\mathcal{N}}_{\mathcal{Z}}(\bar{z})$ such that $\langle z - \bar{z}, v \rangle > 0$. Using Proposition A.1, we have that for any $\bar{\epsilon} > 0$ small enough $v \in \hat{\mathcal{N}}_{\mathcal{Z}}(\bar{z})$ is equivalent to $\langle v, u - \bar{z} \rangle \leq 0$ for all $u \in \mathcal{Z}^i$, and all $i \in \mathcal{I}_{\mathcal{Z}}(\bar{z})$. However, since $z \in \mathcal{Z}$, there exists an $i \in \mathcal{I}_{\mathcal{Z}}(\bar{z})$ such that $z \in \mathcal{Z}^i$, and therefore, by choosing $u = z$, we have $\langle v, u - \bar{z} \rangle < \langle z - \bar{z}, v \rangle$, a contradiction. Furthermore for any $\epsilon \in (0, \bar{\epsilon}]$ we can arrive at the same contradiction.

ii) From [31, Corollary 6.21, p. 216] we know that since for any $z \in \mathcal{Z}$, $\hat{\mathcal{N}}_{\mathcal{Z}}(z)$ is closed and convex we have that $\hat{\mathcal{N}}_{\mathcal{Z}}(z) = \hat{\mathcal{N}}_{\mathcal{Z}}^{**}(z)$. Using (16a), (16b) and convexity of $\hat{\mathcal{N}}_{\mathcal{Z}}^*(z)$ we have that $v \in \hat{\mathcal{N}}_{\mathcal{Z}}(z)$ is equivalent to

$$\begin{aligned} \langle v, w \rangle &\leq 0, & \forall w \in \hat{\mathcal{N}}_{\mathcal{Z}}^*(z) \\ \Leftrightarrow \langle v, u - z \rangle &\leq 0, & \forall u \in \hat{\mathcal{N}}_{\mathcal{Z}}^*(z) + \{z\} \\ \Leftrightarrow v \in \hat{\mathcal{N}}_{\hat{\mathcal{N}}_{\mathcal{Z}}^*(z) + \{z\}}(z). & & \square \end{aligned}$$

Proof of Proposition 2 Given any local optimum z° and $\bar{\xi} > 0$. We show that, the sets $\text{fix } T_\xi|_{z^\circ}$ can only grow with growing ξ . This means that the set $\text{fix } T_\xi|_{z^\circ}$ either (i) remains empty for all ξ , (ii) acquires a single element for some ξ and stays a singleton for all larger ξ , or (iii) does not stay a singleton. Given a $\bar{\xi}$ and $\xi \geq \bar{\xi}$, we will show that for any element $\bar{s} \in \text{fix } T_{\bar{\xi}}|_{z^\circ}$ there, uniquely, exists an element $s \in \text{fix } T_\xi|_{z^\circ}$. Consider any $\bar{s} \in \text{fix } T_{\bar{\xi}}|_{z^\circ}$, by definition and Lemma 2, it holds that (z°, λ) , with $\lambda := \xi(z^\circ - \bar{s})$, is a $\bar{\xi}$ -proximal KKT point. From Proposition 1, it further follows that (z°, λ) is also a ξ -proximal KKT point for any $\xi \geq \bar{\xi}$. Therefore, by definition, $s := z^\circ - \frac{1}{\xi} \lambda \in \text{fix } T_\xi|_{z^\circ}$. This means the sets $\text{fix } T_\xi|_{z^\circ}$ can only grow with larger ξ , and the result follows. \square

The following proposition is an auxiliary proposition needed to prove Lemma 4. It gives a local characterization of the projection around points \bar{s} where it is unique. It states, that there always exists a neighborhood $\mathcal{B}_\epsilon(\bar{s})$, with $\epsilon > 0$, such that for all points in the neighborhood the projection onto \mathcal{Z} can be restricted to the projection onto just the union of the active components of \mathcal{Z} at $\bar{z} := \mathcal{P}_{\mathcal{Z}}(\bar{s})$. Furthermore for all points $s \in \mathcal{B}_\epsilon(\bar{s})$ in the neighborhood the result $z \in \mathcal{P}_{\mathcal{Z}}(s)$ of the projection satisfies the bound $\|z - \bar{z}\| \leq \|s - \bar{s}\|$, i.e., the projection is locally non-expansive with respect to points where it is unique.

Proposition A.2 (Projection) *Given \bar{z} and \bar{s} such that $\mathcal{P}_{\mathcal{Z}}(\bar{s}) = \{\bar{z}\}$, then there exists an $\epsilon > 0$ such that for all $s \in \mathcal{B}_\epsilon(\bar{s})$*

$$\mathcal{P}_{\mathcal{Z}}(s) = \mathcal{P}_{\mathcal{Y}(\bar{z})}(s) \subseteq \mathcal{B}_{\|s - \bar{s}\|}(\bar{z}), \quad (\text{A.4})$$

where

$$\mathcal{Y}(z) := \bigcup_{i \in \mathcal{I}_{\mathcal{Z}}(z)} \mathcal{Z}^i.$$

PROOF. First, we will show that for all $s \in \mathbb{R}^n$

$$\mathcal{P}_{\mathcal{Y}(\bar{z})}(s) \subseteq \mathcal{B}_{\|s - \bar{s}\|}(\bar{z}). \quad (\text{A.5a})$$

We have that for all $i \in \mathcal{I}_{\mathcal{Z}}(\bar{z})$, the projection $\mathcal{P}_{\mathcal{Z}^i}$ is non-expansive because \mathcal{Z}^i is closed and convex, therefore for any $i \in \mathcal{I}_{\mathcal{Z}}(\bar{z})$ and any $s \in \mathbb{R}^n$

$$\|\mathcal{P}_{\mathcal{Z}^i}(s) - \mathcal{P}_{\mathcal{Z}^i}(\bar{s})\| \leq \|s - \bar{s}\|.$$

We consider any $z \in \mathcal{P}_{\mathcal{Y}(\bar{z})}(s)$. Since \bar{z} and \bar{s} are such that $\mathcal{P}_{\mathcal{Z}}(\bar{s}) = \{\bar{z}\}$ it follows that $\mathcal{P}_{\mathcal{Y}(\bar{z})}(\bar{s}) = \mathcal{P}_{\mathcal{Z}^i}(\bar{s}) = \{\bar{z}\}$ for all $i \in \mathcal{I}_{\mathcal{Z}}(\bar{z})$. In particular for some $i \in \mathcal{I}_{\mathcal{Z}}(\bar{z})$ we have that

$$\|z - \bar{z}\| = \|\mathcal{P}_{\mathcal{Z}^i}(s) - \mathcal{P}_{\mathcal{Z}^i}(\bar{s})\| \leq \|s - \bar{s}\|, \quad (\text{A.5b})$$

which implies (A.5a).

Second, we show that there exists an $\epsilon > 0$ such that for any $y \in \mathcal{Z} \setminus \mathcal{Y}(\bar{z})$

$$\|y - s\| > \|z - s\| \quad \forall s \in \mathcal{B}_\epsilon(\bar{s}), z \in \mathcal{P}_{\mathcal{Y}(\bar{z})}(s). \quad (\text{A.6a})$$

We define

$$\varsigma := \inf_{y \in \mathcal{Z} \setminus \mathcal{Y}(\bar{z})} \|y - \bar{s}\| - \|\bar{z} - \bar{s}\| > 0, \quad (\text{A.6b})$$

by closedness of \mathcal{Z} and \mathcal{Z}^i . The triangle inequality implies that for any $y \in \mathcal{Z} \setminus \mathcal{Y}(\bar{z})$ we have,

$$\|y - \bar{s}\| \leq \|y - s\| + \|s - \bar{s}\|.$$

We choose $\epsilon < \frac{\varsigma}{3}$, which implies

$$\begin{aligned} \|y - s\| &\geq \|y - \bar{s}\| - \|s - \bar{s}\| \\ &\geq \varsigma + \|\bar{z} - \bar{s}\| - \|s - \bar{s}\| \\ &> 3\epsilon + \|\bar{z} - \bar{s}\| - \epsilon, \end{aligned} \quad (\text{A.6c})$$

where in the second step we have used (A.6b), and in the third step we have used $\varsigma > 3\epsilon$ and $\|s - \bar{s}\| \leq \epsilon$. Now we consider any $z \in \mathcal{P}_{\mathcal{Y}(\bar{z})}(s)$, we have via the triangle inequality, that

$$\|z - s\| \leq \|z - \bar{z}\| + \|s - \bar{s}\| + \|\bar{z} - \bar{s}\|$$

and therefore by using (A.5b)

$$\begin{aligned} \|z - s\| &\leq 2\|s - \bar{s}\| + \|\bar{z} - \bar{s}\| \\ &\leq 2\epsilon + \|\bar{z} - \bar{s}\|, \end{aligned}$$

which together with (A.6c) implies (A.6a). (A.5a) and (A.6a) then imply the result. \square

In order to prove Lemma 4, we make the following claim:

Claim 1 *Given Assumptions (A1)–(A2). For any $\xi \geq \bar{\xi}$ and any local minimum z° to Problem (2), with $\text{fix } T_\xi|_{z^\circ} \neq \emptyset$ and $z^\circ \notin \text{fix } T_\xi$, we have that*

$$\mathcal{P}_{\mathcal{Z}}(s^\circ) = \{z^\circ\}, \quad \text{and} \quad (\text{A.7a})$$

$$s^\circ \in \text{relint } \hat{\mathcal{N}}_{\mathcal{Z}}(z^\circ) + \{z^\circ\}, \quad (\text{A.7b})$$

for all fixed points $s^\circ \in \text{fix } T_\xi|_{z^\circ}$, except a measure zero subset.

We will show Claim 1 right after the proof of Lemma 4.

Proof of Lemma 4 We assume that Claim 1 holds, and consider any pair z°, s° satisfying (A.7). We will show that in a neighborhood of s° the projection onto \mathcal{Z} is the same as projecting onto an appropriate closed, convex set. This then implies local firm non-expansiveness, continuity and single-valuedness due to the properties of projections onto closed, convex sets.

Let $\mathcal{B}_\epsilon(s^\circ)$ be a neighborhood of s° , for some $\epsilon > 0$ small enough. We define two linear subspaces $\mathcal{S} := \text{lin}(\hat{\mathcal{N}}_{\mathcal{Z}}(z^\circ))$, the linear subspace spanned by $\hat{\mathcal{N}}_{\mathcal{Z}}(z^\circ)$, and its orthogonal complement \mathcal{S}^\perp . Clearly, for any $s \in \mathcal{B}_\epsilon(s^\circ)$ we can write

$s = s^\circ + u + v$, where $u \in \mathcal{S}$, $v \in \mathcal{S}^\perp$ and $u + v \in \mathcal{B}_\epsilon$. This decomposition allows us to argue about the contribution of u and v successively. We consider $\bar{s} := s^\circ + u$. Due to $\mathcal{P}_{\mathcal{Z}}(s^\circ) = \{z^\circ\}$ and [31, Example 6.16, p. 212], we have $\mathcal{P}_{\mathcal{Z}}(\bar{s}) = \mathcal{P}_{\mathcal{Z}}(s^\circ + u) = \{z^\circ\}$ for all $u \in \mathcal{B}_\epsilon$. Furthermore, due to openness of $\text{relint } \hat{\mathcal{N}}_{\mathcal{Z}}(z^\circ)$ on \mathcal{S} , we have that for $\epsilon > 0$ small enough $\bar{s} := s^\circ + u$ satisfies $\bar{s} \in \text{relint } \hat{\mathcal{N}}_{\mathcal{Z}}(z^\circ) + \{z^\circ\}$ for all $u \in \mathcal{B}_\epsilon$. Therefore instead of considering a pair z°, s° satisfying (A.7), we will consider z°, \bar{s} . Now we look at the contribution of v , i.e., $s = \bar{s} + v$. Similarly to Lemma 3, where we showed that we can replace the regular normal cone of \mathcal{Z} by the normal cone of $\hat{\mathcal{N}}_{\mathcal{Z}}^*(z^\circ) + \{z^\circ\}$, we will now consider the projection onto that set. We do this because in some sense $\hat{\mathcal{N}}_{\mathcal{Z}}^*(z^\circ) + \{z^\circ\}$ is a local convexification of \mathcal{Z} . This projection is equivalent to the following optimization problem

$$d^* := \min_{z \in \hat{\mathcal{N}}_{\mathcal{Z}}^*(z^\circ) + \{z^\circ\}} \|s - z\|^2 \quad (\text{A.8a})$$

$$= \min_{\Delta z \in \hat{\mathcal{N}}_{\mathcal{Z}}^*(z^\circ)} \|\bar{s} + v - (\Delta z + z^\circ)\|^2 \quad (\text{A.8b})$$

$$= \min_{\Delta z \in \hat{\mathcal{N}}_{\mathcal{Z}}^*(z^\circ)} \|\bar{s} - z^\circ\|^2 + \|v - \Delta z\|^2 + 2\langle \bar{s} - z^\circ, v - \Delta z \rangle \quad (\text{A.8c})$$

Due to $\bar{s} - z^\circ \in \hat{\mathcal{N}}_{\mathcal{Z}}(z^\circ) \subseteq \mathcal{S}$ and $v \in \mathcal{S}^\perp$ we have $\langle \bar{s} - z^\circ, v \rangle = 0$. Furthermore by definition of $\hat{\mathcal{N}}_{\mathcal{Z}}^*(z^\circ)$ we have $\langle \Delta z, \bar{s} - z^\circ \rangle \leq 0$. Therefore, using Assumption (A3), i.e., $z^\circ + v \in \mathcal{Z}$, for ϵ small enough, and Lemma 3 we have $v \in \hat{\mathcal{N}}_{\mathcal{Z}}^*(z^\circ)$ which leads to

$$d^* \geq \min_{\Delta z \in \hat{\mathcal{N}}_{\mathcal{Z}}^*(z^\circ)} \|\bar{s} - z^\circ\|^2 + \|v - \Delta z\|^2 = \|\bar{s} - z^\circ\|^2.$$

Furthermore, using $v \in \hat{\mathcal{N}}_{\mathcal{Z}}^*(z^\circ)$ and choosing $\Delta z = v$ we get $d^* \leq \|\bar{s} - z^\circ\|^2$ from (A.8), simply via feasibility. This implies that $d^* = \|\bar{s} - z^\circ\|^2$, which due to strict convexity of Problem (A.8) implies that

$$\mathcal{P}_{\hat{\mathcal{N}}_{\mathcal{Z}}^*(z^\circ) + \{z^\circ\}}(\bar{s} + v) = \{z^\circ + v\}.$$

Additionally, due to $\mathcal{Z} \cap \mathcal{B}_\epsilon(z^\circ) \subseteq \hat{\mathcal{N}}_{\mathcal{Z}}^*(z^\circ) + \{z^\circ\}$ from Lemma 3 and $z^\circ + v \in \mathcal{Z} \cap \mathcal{B}_\epsilon(z^\circ)$ due to Assumption (A3), it follows that $\{z^\circ + v\} \in \mathcal{P}_{\mathcal{Z}}(\bar{s} + v)$. Finally using Proposition A.2 we know that

$$\mathcal{P}_{\mathcal{Z}}(\bar{s} + v) \subseteq \mathcal{Z} \cap \mathcal{B}_{\|v\|}(z^\circ) \subseteq \mathcal{Z} \cap \mathcal{B}_\epsilon(z^\circ),$$

which immediately implies that

$$\mathcal{P}_{\mathcal{Z}}(\bar{s} + v) = \mathcal{P}_{\hat{\mathcal{N}}_{\mathcal{Z}}^*(z^\circ) + \{z^\circ\}}(\bar{s} + v) = \{z^\circ + v\}.$$

This means for all $s \in \mathcal{B}_\epsilon(s^\circ)$ the projection onto \mathcal{Z} is equivalent to the projection onto the closed, convex set $\hat{\mathcal{N}}_{\mathcal{Z}}^*(z^\circ) + \{z^\circ\}$ and therefore enjoys all of the properties of a projection onto a closed convex set. In particular single-valuedness, continuity and firm non-expansiveness [40, Proposition 4.8, p. 61]. \square

Proof of Claim 1 Given a $\xi > \bar{\xi}$ and local minimum z° to Problem (2), we define the auxiliary set $\mathcal{C}_\xi(z^\circ)$ of fixed points corresponding to z° , where (A.7) is violated

$$\mathcal{C}_\xi(z^\circ) := \{s \in \text{fix } T_\xi|_{z^\circ} \mid s \notin \text{relint } \hat{\mathcal{N}}_{\mathcal{Z}}(z^\circ) + \{z^\circ\}, \text{ or } \mathcal{P}_{\mathcal{Z}}(s) \neq \{z^\circ\}\}.$$

We want to show that for any $\xi > \bar{\xi}$, and any local minimum z° such that $\text{fix } T_\xi|_{z^\circ} \neq \emptyset$, the set $\mathcal{C}_\xi(z^\circ)$ is a measure-zero subset of $\text{fix } T_\xi|_{z^\circ}$. This then implies that (A.7a) and (A.7b) hold for all $s \in \text{fix } T_\xi|_{z^\circ}$ except a measure-zero subset. We consider the two cases:

First, we consider the case where, given a local minimum z° , $\text{fix } T_\xi|_{z^\circ}$ is a singleton set for all $\xi \geq \bar{\xi}$. In particular there exists an s° such that $\{s^\circ\} = \text{fix } T_{\bar{\xi}}|_{z^\circ}$, which by definition implies that $z^\circ \in \mathcal{P}_{\mathcal{Z}}(s^\circ)$. Via [31, Example 6.16, p. 212], this further implies that $\{z^\circ\} = \mathcal{P}_{\mathcal{Z}}(s(\xi))$ for all $\xi > \bar{\xi}$, where $s(\xi) := z^\circ - \frac{1}{\xi}(z^\circ - s^\circ)$, and $\{s(\xi)\} = \text{fix } T_\xi|_{z^\circ}$, by definition and Assumption (A2). Furthermore, by Assumption (A2), we have that for all $\xi \geq \bar{\xi}$, it holds that $s(\xi) \in \text{relint } \hat{\mathcal{N}}_{\mathcal{Z}}(z^\circ) + \{z^\circ\}$. Therefore, for all $\xi > \bar{\xi}$, we have that $\mathcal{C}_\xi(z^\circ) = \emptyset$.

Next we consider the case where, given a local minimum z° , $\text{fix } T_\xi|z^\circ$ contains more than one element for all $\xi \geq \bar{\xi}$. We define the sets

$$\begin{aligned}\mathcal{C}_\xi^{\mathcal{N}}(z^\circ) &:= \{s \in \text{fix } T_\xi|z^\circ \mid s \in \text{relbd } \hat{\mathcal{N}}_{\mathcal{Z}}(z^\circ) + \{z^\circ\}\}, \\ \mathcal{C}_\xi^{\mathcal{P}}(z^\circ) &:= \{s \in \text{fix } T_\xi|z^\circ \mid \mathcal{P}_{\mathcal{Z}}(s) \neq \{z^\circ\}\},\end{aligned}$$

with $\mathcal{C}_\xi(z^\circ) = \mathcal{C}_\xi^{\mathcal{N}}(z^\circ) \cup \mathcal{C}_\xi^{\mathcal{P}}(z^\circ)$. We will show that the sets $\mathcal{C}_\xi^{\mathcal{N}}(z^\circ)$ and $\mathcal{C}_\xi^{\mathcal{P}}(z^\circ)$ are measure-zero subsets of $\text{fix } T_\xi|z^\circ$, which implies that $\mathcal{C}_\xi(z^\circ)$ is a measure-zero subset of $\text{fix } T_\xi|z^\circ$.

We first consider the set $\mathcal{C}_\xi^{\mathcal{N}}(z^\circ)$, which is defined as the union of all the facets of the shifted closed convex polyhedral cone $\hat{\mathcal{N}}_{\mathcal{Z}}(z^\circ) + \{z^\circ\}$ intersected with the convex set $\text{fix } T_\xi|z^\circ$. The cone $\hat{\mathcal{N}}_{\mathcal{Z}}(z^\circ)$ is finitely generated and therefore has a finite number of facets. By Assumption (A2) we know that there exists a $\bar{s} \in \text{fix } T_\xi|z^\circ$ such that $\bar{s} \in \text{relint } \hat{\mathcal{N}}_{\mathcal{Z}}(z^\circ) + \{z^\circ\}$. Therefore, for each facet \mathcal{F} of $\hat{\mathcal{N}}_{\mathcal{Z}}(z^\circ)$, by convexity of $\text{fix } T_\xi|z^\circ$, we have that $\text{conv}((\mathcal{F} \cap \text{fix } T_\xi|z^\circ) \cup \{\bar{s}\}) \subseteq \text{fix } T_\xi|z^\circ$ and that $\mathcal{F} \cap \text{fix } T_\xi|z^\circ$ is a measure-zero subset of $\text{conv}((\mathcal{F} \cap \text{fix } T_\xi|z^\circ) \cup \{\bar{s}\})$ by virtue of the fact that $\bar{s} \notin \mathcal{F}$. This immediately implies that $\mathcal{F} \cap \text{fix } T_\xi|z^\circ$ is a measure-zero subset of $\text{fix } T_\xi|z^\circ$ and thereby $\mathcal{C}_\xi^{\mathcal{N}}(z^\circ)$ is a measure-zero subset of $\text{fix } T_\xi|z^\circ$.

Now we consider the set $\mathcal{C}_\xi^{\mathcal{P}}(z^\circ)$. Again by convexity of $\text{fix } T_\xi|z^\circ$ we know that the relative boundary $\text{relbd}(\text{fix } T_\xi|z^\circ)$ of $\text{fix } T_\xi|z^\circ$ is a measure zero subset of $\text{fix } T_\xi|z^\circ$. We will show that $\mathcal{C}_\xi^{\mathcal{P}}(z^\circ) \subseteq \text{relbd}(\text{fix } T_\xi|z^\circ)$. For the sake of arriving at a contradiction, we assume that there exists a $s \in \text{relint}(\text{fix } T_\xi|z^\circ)$ such that there exists a $\bar{z} \neq z^\circ$, with $\{z^\circ, \bar{z}\} \subseteq \mathcal{P}_{\mathcal{Z}}(s)$. By openness and convexity of $\text{relint}(\text{fix } T_\xi|z^\circ)$ there exists a $d \in \mathbb{R}^n$ and $\bar{\epsilon} > 0$, with $\|d\| = 1$ such that $s + \theta d \in \text{fix } T_\xi|z^\circ$ for all $\theta \in [-\bar{\epsilon}, \bar{\epsilon}]$. By definition we have that $z^\circ \in \mathcal{P}_{\mathcal{Z}}(s + \theta d)$ and therefore $\|s + \theta d - z^\circ\| \leq \|s + \theta d - z\|$ for all $\theta \in [-\bar{\epsilon}, \bar{\epsilon}]$ and $z \in \mathcal{Z}$. Because $\|s - z^\circ\| = \|s - \bar{z}\|$, we in fact have $0 = \|s - z^\circ\|^2 - \|s - \bar{z}\|^2 \leq \theta(z^\circ - \bar{z}, d)$ for all $\theta \in [-\bar{\epsilon}, \bar{\epsilon}]$, a contradiction. Therefore $\mathcal{C}_\xi^{\mathcal{P}}(z^\circ) \subseteq \text{relbd}(\text{fix } T_\xi|z^\circ)$, which implies that the set $\mathcal{C}_\xi^{\mathcal{P}}(z^\circ)$ is also a measure-zero subset of $\text{fix } T_\xi|z^\circ$ and therefore $\mathcal{C}_\xi(z^\circ)$ is a measure-zero subset of $\text{fix } T_\xi|z^\circ$. This means that (A.7) holds for all $s \in \text{fix } T_\xi|z^\circ$ except a measure-zero subset. \square

Proof of Lemma 5 We consider any $\xi > 0$ and $s^\circ \in \text{fix } T_\xi$ such that there exists an $\epsilon > 0$ such that the projection $\mathcal{P}_{\mathcal{Z}}$ is single-valued, continuous and firmly non-expansive on $\mathcal{B}_\epsilon(s^\circ)$. We recall the definition of T_ξ in (14b). Clearly T_ξ is single-valued and continuous on $\mathcal{B}_\epsilon(s^\circ)$ by virtue of the projection. It remains to show the non-expansiveness of T_ξ on $\mathcal{B}_\epsilon(s^\circ)$. By [40, Definition 4.1 (ii), p. 59] T_ξ is non-expansive on $\mathcal{B}_\epsilon(s^\circ)$ if

$$\|T_\xi(s) - T_\xi(t)\|^2 \leq \|s - t\|^2, \quad \forall s, t \in \mathcal{B}_\epsilon(s^\circ).$$

For any s, t , we have by definition of T_ξ , that

$$\begin{aligned}\|T_\xi(s) - T_\xi(t)\|^2 &= \|(I - WM_\xi)(s - t)\|^2 + 2\langle W^\top(I - WM_\xi)(s - t), \mathcal{P}_{\mathcal{Z}}(s) - \mathcal{P}_{\mathcal{Z}}(t) \rangle \\ &\quad + \|W(\mathcal{P}_{\mathcal{Z}}(s) - \mathcal{P}_{\mathcal{Z}}(t))\|^2.\end{aligned}\tag{A.10}$$

In order to show that (A.10) $\leq \|s - t\|^2$ for all $s, t \in \mathcal{B}_\epsilon(s^\circ)$ we are going to split (A.10) into two parts, the portions belonging to the range- and nullspace of M_ξ . We recall that M_ξ is positive semi-definite for ξ satisfying (12a). Therefore, we can consider the eigenvalue decomposition of M_ξ , as in (14) and define q_i , for $i = 1, \dots, n$, to be the normalized eigenvectors of M_ξ . We define $\delta, p \in \mathbb{R}^n$ as the coefficients of linear combinations of the eigenvectors of M_ξ , such that $\sum_{i=1}^n \delta_i q_i = s - t$ and $\sum_{i=1}^n p_i q_i = \mathcal{P}_{\mathcal{Z}}(s) - \mathcal{P}_{\mathcal{Z}}(t)$. We further define

$$\begin{aligned}\delta^\perp &:= \sum_{i=1}^{n-m} \delta_i q_i, & \delta^0 &:= \sum_{i=n-m+1}^n \delta_i q_i, \\ p^\perp &:= \sum_{i=1}^{n-m} p_i q_i, \text{ and} & p^0 &:= \sum_{i=n-m+1}^n p_i q_i,\end{aligned}$$

which splits $s - t$ and $\mathcal{P}_{\mathcal{Z}}(s) - \mathcal{P}_{\mathcal{Z}}(t)$ into their range and nullspace portions. Substituting $\delta^\perp, \delta^0, p^\perp$ and p^0 into (A.10), using the eigenvalue decomposition of M_ξ and W as defined in (14d), we obtain

$$\|T_\xi(s) - T_\xi(t)\|^2 = \frac{1}{4}\|\delta^\perp\|^2 + \|\delta^0\|^2 + \frac{1}{2}\langle\delta^\perp, p_\Lambda^\perp\rangle - 2\langle\delta^0, p^0\rangle + \frac{1}{4}\|p_\Lambda^\perp\|^2 + \|p^0\|^2, \quad (\text{A.12})$$

where $p_\Lambda^\perp := \sum_{i=1}^{n-m} \lambda_i^{-1} p_i q_i$ for λ_i the non-zero eigenvalues of M_ξ . We want to show that (A.12) $\leq \|s - t\|^2 = \|\delta^\perp\|^2 + \|\delta^0\|^2$. However, this only has to hold for δ, p that are related via the projection $\mathcal{P}_{\mathcal{Z}}$ where in particular we want to exploit its firm non-expansiveness. The projection $\mathcal{P}_{\mathcal{Z}}$ being firmly non-expansive on $\mathcal{B}_\epsilon(s^\circ)$, means by [40, Proposition 4.2 (iv), p. 60], that for all $s, t \in \mathcal{B}_\epsilon(s^\circ)$

$$\|\mathcal{P}_{\mathcal{Z}}(s) - \mathcal{P}_{\mathcal{Z}}(t)\|^2 \leq \langle s - t, \mathcal{P}_{\mathcal{Z}}(s) - \mathcal{P}_{\mathcal{Z}}(t) \rangle. \quad (\text{FNE})$$

Furthermore, it is also non-expansive, i.e., for any $s, t \in \mathcal{B}_\epsilon(s^\circ)$

$$\|\mathcal{P}_{\mathcal{Z}}(s) - \mathcal{P}_{\mathcal{Z}}(t)\|^2 \leq \|s - t\|^2, \quad (\text{NE})$$

By applying the Cauchy-Schwarz inequality, and combining (FNE) and (NE) we finally get

$$0 \leq \|\mathcal{P}_{\mathcal{Z}}(s) - \mathcal{P}_{\mathcal{Z}}(t)\|^2 \leq \langle s - t, \mathcal{P}_{\mathcal{Z}}(s) - \mathcal{P}_{\mathcal{Z}}(t) \rangle \leq \|s - t\|^2. \quad (\text{A.13})$$

We can also substitute $\delta^\perp, \delta^0, p^\perp$ and p^0 into (A.13) obtaining

$$0 \leq \|p^\perp\|^2 + \|p^0\|^2 \leq \langle p^\perp, \delta^\perp \rangle + \langle p^0, \delta^0 \rangle \leq \|\delta^\perp\|^2 + \|\delta^0\|^2. \quad (\text{A.14})$$

To show that T_ξ is non-expansive it is therefore sufficient to show that for all δ, p that satisfy (A.14) it holds that (A.12) $\leq \|\delta^\perp\|^2 + \|\delta^0\|^2$. Notice, that (A.12) and (A.14) do not contain any coupling terms between range- and nullspace portions of δ or p , therefore we can argue about them separately.

i) We want to show that for all δ^\perp, p^\perp such that

$$0 \leq \|p^\perp\|^2 \leq \langle p^\perp, \delta^\perp \rangle \leq \|\delta^\perp\|^2, \quad (\text{A.15a})$$

we have that

$$\frac{1}{4}\|\delta^\perp\|^2 + \frac{1}{2}\langle\delta^\perp, p_\Lambda^\perp\rangle + \frac{1}{4}\|p_\Lambda^\perp\|^2 \leq \|\delta^\perp\|^2.$$

Given p^\perp, δ^\perp such that (A.15a) holds, using (12b) implies that $\|\Lambda^{-1}\|_2 \leq 1$ thus we obtain $\|p_\Lambda^\perp\| \leq \|p^\perp\| \leq \|\delta^\perp\|$ and $\langle\delta^\perp, p_\Lambda^\perp\rangle \leq \|\delta^\perp\|^2$. Therefore

$$\frac{1}{4}\|\delta^\perp\|^2 + \frac{1}{2}\langle\delta^\perp, p_\Lambda^\perp\rangle + \frac{1}{4}\|p_\Lambda^\perp\|^2 \leq \frac{1}{4}\|\delta^\perp\|^2 + \frac{1}{2}\|\delta^\perp\|^2 + \frac{1}{4}\|\delta^\perp\|^2 = \|\delta^\perp\|^2.$$

ii) We want to show that for all δ^0, p^0 such that

$$0 \leq \|p^0\|^2 \leq \langle p^0, \delta^0 \rangle \leq \|\delta^0\|^2,$$

we have that

$$\|\delta^0\|^2 - 2\langle\delta^0, p^0\rangle + \|p^0\|^2 \leq \|\delta^0\|^2.$$

We consider

$$\|\delta^0\|^2 - 2\langle\delta^0, p^0\rangle + \|p^0\|^2 \leq \|\delta^0\|^2 - 2\langle\delta^0, p^0\rangle + \langle\delta^0, p^0\rangle \leq \|\delta^0\|^2.$$

Cases i) and ii) together imply the result. \square

B Algorithm for checking (A3)

In this section we give an algorithm for checking Assumption (A3). The assumption is purely geometrical and needs to be satisfied at every point in \mathcal{Z} . Therefore the algorithm will effectively enumerate all possible combinations of active components and their active sets and check for each such combination. This amounts to a finite (but combinatorial) number of checks. Note that checking a parametric set $\mathcal{Z}(\theta)$, due to the polyhedral structure, amounts to checking finitely many different non-parametric sets. Therefore $\mathcal{Z}(\theta)$ can be checked once and “offline” for all θ .

We begin by defining the *active set* $\mathcal{J}_{\mathcal{Z}(\theta)}(z)$ of $\mathcal{Z}(\theta)$, with parameter $\theta \in \mathbb{R}^p$, at $z \in \mathcal{Z}$, as the collection of all the active sets of the components of $\mathcal{Z}(\theta)$

$$\mathcal{J}_{\mathcal{Z}(\theta)}(z) := \{\mathcal{J}_{\mathcal{Z}^i(\theta)}(z)\}_{i=1}^I,$$

where the active set $\mathcal{J}_{\mathcal{Z}^i(\theta)}(z)$ of a polyhedron $\mathcal{Z}^i(\theta)$ is defined in the usual way [28, Definition 12.1, p. 308] as the set of constraints active at $z \in \mathcal{Z}^i(\theta)$ and $\mathcal{J}_{\mathcal{Z}^i(\theta)}(z) = \emptyset$ if $z \notin \mathcal{Z}^i(\theta)$. The set $\mathcal{I}_{\mathcal{Z}} \subseteq 2^{\{1, \dots, I\}}$ denotes the set of sets of active components of $\mathcal{Z}(\theta)$, i.e., $\mathcal{I} \in \mathcal{I}_{\mathcal{Z}(\theta)}$ if and only if there exists θ and $z \in \mathcal{Z}(\theta)$ such that $\mathcal{I} \equiv \mathcal{I}_{\mathcal{Z}(\theta)}(z)$. Similarly we denote by $\mathcal{J}_{\mathcal{Z}(\theta)}$ the set of all possible active sets of $\mathcal{Z}(\theta)$

$$\mathcal{J}_{\mathcal{Z}(\theta)} := \left\{ \{\mathcal{J}_i\}_{i=1}^I \mid \exists \theta \in \mathbb{R}^p, \exists z \in \mathcal{Z}(\theta) \text{ s. t. } \{\mathcal{J}_i\}_{i=1}^I \equiv \mathcal{J}_{\mathcal{Z}(\theta)}(z) \right\},$$

We will consider $\mathcal{Z}(\theta)$ with components $\mathcal{Z}^i(\theta)$ defined as

$$\mathcal{Z}(\theta) = \bigcup_{i=1}^I \underbrace{\{z \mid F^i z \leq f^i(\theta), G^i z = g^i(\theta)\}}_{\mathcal{Z}^i(\theta)}, \quad (\text{B.2})$$

where $F^i \in \mathbb{R}^{m_i \times n}$, $G^i \in \mathbb{R}^{p_i \times n}$ and $f^i \in \mathbb{R}^{m_i}$. The functions $f^i(\theta) = F^{i,\theta}\theta + f^i$ and $g^i(\theta) = G^{i,\theta}\theta + g^i$ depend affinely on a parameter $\theta \in \mathbb{R}^p$. With $\mathcal{Z}^i(\theta)$ closed convex polyhedra for fixed θ and non-empty for some θ . Given a component i and one of its active sets \mathcal{J}_i , then $F_{\mathcal{J}_i}^i$ denotes the subset of rows of F^i that belong to the active set \mathcal{J}_i , $f_{\mathcal{J}_i}^i$ is defined in the same way.

Algorithm 3 Check of Assumption (A3)

Require: $\mathcal{Z}(\theta)$ as in (B.2)

```

1: for each  $\mathcal{I} \in \mathcal{I}_{\mathcal{Z}(\theta)}$ ,  $\{\mathcal{J}_i\}_{i=1}^I \in \mathcal{J}_{\mathcal{Z}(\theta)}$  do
2:    $\mathcal{N} \leftarrow \bigcap_{i \in \mathcal{I}} \{v \mid v = (F_{\mathcal{J}_i}^i)^\top \mu + (G^i)^\top \nu, \mu \geq 0\}$ 
3:   if  $\mathcal{N} = \{0\}$  then
4:     continue
5:   for each  $i \in \mathcal{I}$  do
6:      $\mathcal{R}_i = \{v \mid F_{\mathcal{J}_i}^i v \leq 0, G^i v = 0\}$ 
7:    $\mathcal{R} \leftarrow \bigcup_{i \in \mathcal{I}} \mathcal{R}_i$ 
8:   if  $\mathcal{N}^\perp \subseteq \mathcal{R}$  then
9:     continue
10:  else
11:     $w \leftarrow w \in \mathcal{N}^\perp \setminus \mathcal{R}$ 
12:    return  $(w, \{\mathcal{A}_j\}_{j=1}^m)$ 

```

▷ Counter-example

Lemma B.1 *Give a (parametric) set $\mathcal{Z}(\theta)$ as in (B.2), then Algorithm 3 terminates in a finite number of steps. Either $\mathcal{Z}(\theta)$ satisfies Assumption (A3) for all θ , or the algorithm returns a valid counter-example.*

Algorithm 3 is a combinatorial algorithm and may perform badly for anything but small dimensions. However, since by assumption the set \mathcal{Z} is a Cartesian product of sets in low dimension, the check can be performed separately for each part of the Cartesian product. This significantly reduces the “curse of dimensionality”. Furthermore this analysis can be performed once and “offline”.

Proof of Lemma B.1 We will show that Algorithm 3 effectively checks Assumption (A3) for every θ and every point in $\mathcal{Z}(\theta)$. We will argue, that checking (A3) for every $\theta \in \mathbb{R}^p$ and every $z \in \mathcal{Z}(\theta)$ is equivalent to checking it for

every set of active constraints. Note that $\mathcal{A}_{\mathcal{Z}(\theta)}$ the set of active sets of $\mathcal{Z}(\theta)$ is a finite set with at most $2^{\bar{m}}$ elements, where $\bar{m} := \sum_{i=1}^I m_i$. We further note that $\mathcal{I}_{\mathcal{Z}(\theta)}$ and $\mathcal{J}_{\mathcal{Z}(\theta)}$ can be constructed by solving a finite number of linear programs.

In Algorithm 3, we iterate over the elements of $\mathcal{I}_{\mathcal{Z}(\theta)}$ and $\mathcal{J}_{\mathcal{Z}(\theta)}$, which means that the loop is executed at most a finite number of times. For each pair $\mathcal{I}, \{\mathcal{J}_i\}_{i=1}^I$ we want to verify, or invalidate, (A3) by looking at two sets \mathcal{N} and \mathcal{R} , these set are defined solely via the active constraints and do not depend on θ , since θ only affects the sets $\mathcal{I}_{\mathcal{Z}(\theta)}$ and $\mathcal{J}_{\mathcal{Z}(\theta)}$. Given a pair $\mathcal{I}, \{\mathcal{J}_i\}_{i=1}^I$, for each active component $i \in \mathcal{I}$ we can define two auxiliary sets

$$\begin{aligned} \mathcal{A}_i(\theta) &:= \{z \mid F_{\mathcal{J}_i}^i z = f_{\mathcal{J}_i}^i(\theta), F_{\mathcal{J}_i^c}^i z < f_{\mathcal{J}_i^c}^i(\theta), G^i z = g^i(\theta)\}, \\ \mathcal{F}_i(\theta) &:= \{z \mid F_{\mathcal{J}_i}^i z \leq f_{\mathcal{J}_i}^i(\theta), G^i z = g^i(\theta)\}, \end{aligned}$$

where the set \mathcal{J}_i^c is simply the complement of \mathcal{J}_i , i.e., the set of constraints that are not active. For a given θ , set $\mathcal{A}_i(\theta)$ is the set of points $z \in \mathcal{Z}$ that belong to the active set \mathcal{J}_i , whereas $\mathcal{F}_i(\theta) \supseteq \mathcal{A}_i(\theta)$ is a larger set, that is defined by only the active constraints and in general is not included in \mathcal{Z} . For a pair $\mathcal{I}, \{\mathcal{J}_i\}_{i=1}^I$ we can further define $\mathcal{A}(\theta) := \bigcap_{i=1}^I \mathcal{A}_i(\theta)$, the set of points that belong to all of the active sets of the active components. By checking Assumption (A3) for each $\mathcal{A}(\theta)$ we will effectively check it for each $z \in \mathcal{Z}$.

The conditions to be checked involve the regular normal cone $\hat{\mathcal{N}}_{\mathcal{Z}(\theta)}(z)$. For each $\theta, z \in \mathcal{A}(\theta)$ we can fully characterize the regular normal cone $\hat{\mathcal{N}}_{\mathcal{Z}(\theta)}(z)$, using Proposition A.1 and [31, Theorem 6.46, p. 231]

$$\hat{\mathcal{N}}_{\mathcal{Z}(\theta)}(z) = \bigcap_{i \in \mathcal{I}} \{(F_{\mathcal{J}_i}^i)^\top \mu + (G^i)^\top \nu \mid \mu \geq 0\}.$$

We see that $\hat{\mathcal{N}}_{\mathcal{Z}(\theta)}(z)$ is independent of θ and z , it only depends on which constraints (and components) are active. This set, $\mathcal{N} := \hat{\mathcal{N}}_{\mathcal{Z}(\theta)}(z)$, is computed in step 2 of Algorithm 3. A half-space representation of \mathcal{N} can be obtained using Fourier-Motzkin elimination [44, p. 84] for each i , after which the intersections are trivial. We now need to check two conditions. If \mathcal{N} is equivalent to $\{0\}$, then the first part of (A3) is satisfied for all $z \in \mathcal{A}(\theta)$, and we continue with the next active set. Otherwise we need to check whether there exists an $\epsilon > 0$ such that for all $w \in \mathcal{N}^\perp \cap \mathcal{B}_\epsilon$ we have that $z + w \in \mathcal{Z}(\theta)$. In order to check this condition, in steps 6–7, we construct the set \mathcal{R} as the union of the recession cones $\mathcal{R}_i := \text{rec}(\mathcal{F}_i(\theta))$ of $\mathcal{F}_i(\theta)$. Finally it remains to show that checking this condition for all $z \in \mathcal{A}(\theta)$, in step 8, is equivalent to checking whether the orthogonal complement $\mathcal{N}^\perp := \{v \in \mathbb{R}^n \mid \langle v, u \rangle = 0, \forall u \in \mathcal{N}\}$ is contained in \mathcal{R} . If $\mathcal{N}^\perp \subseteq \mathcal{R}$, consider any $z \in \mathcal{A}(\theta)$, an $\epsilon > 0$ small enough and any $w \in \mathcal{N}^\perp \cap \mathcal{B}_\epsilon$. Clearly there exists an $i \in \mathcal{I}$ such that $w \in \mathcal{R}_i$. Furthermore, by construction of $\mathcal{A}(\theta)$ and \mathcal{R}_i , we have $z + w \in \mathcal{Z}^i \subseteq \mathcal{Z}$, which can be verified simply by checking that the constraints of \mathcal{Z}^i are not violated.

If \mathcal{R} does not contain \mathcal{N}^\perp , then there exists a $w \in \mathcal{N}^\perp$ such that $w \notin \mathcal{R}_i$, for all $i \in \mathcal{I}$. Because \mathcal{N} and \mathcal{R}_i are cones, this is true for all positive scalings of w . In particular, for any $\epsilon > 0$ there exists a $\nu > 0$ such that $\nu w \in \mathcal{N}^\perp \cap \mathcal{B}_\epsilon$ and $\nu w \notin \mathcal{R}$. Analogously to above, it follows that for any $z \in \mathcal{A}(\theta)$, $z + \nu w \notin \mathcal{Z}^i$ for all $i \in \mathcal{I}$, and therefore $z + \nu w \notin \mathcal{Z}$, which violates (A3). Then, the algorithm terminates and returns a violating direction w and the corresponding active set, from which violating z, θ can be reconstructed. Because the Algorithm 3 enumerates all active sets, it either terminates with a counterexample, or it returns after finitely many steps, having checked all possibilities. \square

References

- [1] F. Borrelli, A. Bemporad, M. Fodor, and D. Hrovat, “An MPC/hybrid system approach to traction control,” *IEEE Transactions on Control Systems Technology*, vol. 14, no. 3, pp. 541–552, 2006.
- [2] S. D. Cairano, A. Bemporad, I. V. Kolmanovskiy, and D. Hrovat, “Model predictive control of magnetically actuated mass spring dampers for automotive applications,” *International Journal of Control*, vol. 80, no. 11, pp. 1701–1716, 2007.
- [3] A. Arce, A. J. del Real, and C. Bordons, “MPC for battery/fuel cell hybrid vehicles including fuel cell dynamics and battery performance improvement,” *Journal of Process Control*, vol. 19, no. 8, pp. 1289–1304, 2009.
- [4] A. Vahidi, A. Stefanopoulou, and H. Peng, “Current management in a hybrid fuel cell power system: A model-predictive control approach,” *IEEE Transactions on Control Systems Technology*, vol. 14, no. 6, pp. 1047–1057, 2006.
- [5] T. Geyer, G. Papafotiou, R. Frasca, and M. Morari, “Constrained optimal control of the step-down dc-dc converter,” *IEEE Transactions on Power Electronics*, vol. 23, no. 5, pp. 2454–2464, 2008.

- [6] M. Morari and J. H. Lee, "Model predictive control: past, present and future," *Computers & Chemical Engineering*, vol. 23, no. 4–5, pp. 667–682, 1999.
- [7] D. Q. Mayne, J. B. Rawlings, C. V. Rao, and P. O. M. Scokaert, "Constrained model predictive control: Stability and optimality," *Automatica*, vol. 36, no. 6, pp. 789–814, 2000.
- [8] J. M. Maciejowski, *Predictive Control: With Constraints*. Prentice Hall, 2002.
- [9] A. Bemporad and M. Morari, "Control of systems integrating logic, dynamics, and constraints," *Automatica*, vol. 35, no. 3, pp. 407–427, 1999.
- [10] International Business Machines Corp. (IBM), "IBM ILOG CPLEX optimization studio." <http://www.ibm.com/software/commerce/optimization/cplex-optimizer>, Dec. 2015.
- [11] Gurobi Optimization, Inc., "Gurobi optimizer reference manual," 2015.
- [12] X. Guan, Z. Xu, and Q.-S. Jia, "Energy-efficient buildings facilitated by microgrid," *IEEE Transactions on Smart Grid*, vol. 1, no. 3, pp. 243–252, 2010.
- [13] Y. Ma, F. Borrelli, B. Hancey, B. Coffey, S. Bengea, and P. Haves, "Model predictive control for the operation of building cooling systems," *IEEE Transactions on Control Systems Technology*, vol. 20, no. 3, pp. 796–803, 2012.
- [14] K. S. Stadler, J. Poland, and E. Gallestey, "Model predictive control of a rotary cement kiln," *Control Engineering Practice*, vol. 19, no. 1, pp. 1–9, 2011.
- [15] D. Frick, A. Domahidi, and M. Morari, "Embedded optimization for mixed logical dynamical systems," *Computers & Chemical Engineering*, vol. 72, pp. 21–33, 2015. A Tribute to Ignacio E. Grossmann.
- [16] D. Axehill, *Integer Quadratic Programming for Control and Communication*. PhD thesis, Linköping University, The Institute of Technology, 2008.
- [17] S. Sager, *Numerical methods for mixed-integer optimal control problems*. PhD thesis, Universität Heidelberg, 2005.
- [18] M. Jung, *Relaxations and Approximations for Mixed-Integer Optimal Control*. PhD thesis, Ruprecht-Karls-Universität Heidelberg, 2013.
- [19] D. Gabay and B. Mercier, "A dual algorithm for the solution of nonlinear variational problems via finite element approximation," *Computers & Mathematics with Applications*, vol. 2, no. 1, pp. 17 – 40, 1976.
- [20] S. Boyd, N. Parikh, E. Chu, B. Peleato, and J. Eckstein, "Distributed optimization and statistical learning via the alternating direction method of multipliers," *Foundations and Trends in Machine Learning*, vol. 3, no. 1, pp. 1–122, 2011.
- [21] J. L. Jerez, P. J. Goulart, S. Richter, G. A. Constantinides, E. C. Kerrigan, and M. Morari, "Embedded online optimization for model predictive control at megahertz rates," *IEEE Transactions on Automatic Control*, vol. 59, pp. 3238–3251, Dec. 2014.
- [22] R. Takapoui, N. Moehle, S. Boyd, and A. Bemporad, "A simple effective heuristic for embedded mixed-integer quadratic programming," *arXiv preprint arXiv:1509.08416*, 2015.
- [23] G. Li and T. K. Pong, "Global convergence of splitting methods for nonconvex composite optimization," *SIAM Journal on Optimization*, vol. 25, no. 4, pp. 2434–2460, 2015.
- [24] S. Magnússon, P. C. Weeraddana, M. G. Rabbat, and C. Fischione, "On the convergence of alternating direction lagrangian methods for nonconvex structured optimization problems," *IEEE Transactions on Control of Network Systems*, 2015. accepted.
- [25] J.-H. Hours and C. N. Jones, "A parametric nonconvex decomposition algorithm for real-time and distributed NMPC," *IEEE Transactions on Automatic Control*, vol. 61, no. 2, pp. 287–302, 2016.
- [26] B. Houska, J. Frasch, and M. Diehl, "An augmented Lagrangian based algorithm for distributed non-convex optimization," *Optimization Online*, 2014.
- [27] D. Frick, "Automatic code-generation tool for LIM." <https://github.com/dafrick/codegen>, 2016.
- [28] J. Nocedal and S. J. Wright, *Numerical optimization*. Springer Science+Business Media, 2 ed., 2006.
- [29] MOSEK ApS, *The MOSEK optimization toolbox for MATLAB manual. Version 7.1 (Revision 28)*, 2015.
- [30] A. Ruszczyński, *Nonlinear Optimization*. Princeton University Press, 2006.
- [31] R. T. Rockafellar and R. J.-B. Wets, *Variational analysis*. Springer, 1998.
- [32] J. J. Ye, "Constraint qualifications and necessary optimality conditions for optimization problems with variational inequality constraints," *SIAM Journal on Optimization*, vol. 10, no. 4, pp. 943–962, 2000.
- [33] R. Henrion and J. Outrata, "On calculating the normal cone to a finite union of convex polyhedra," *Optimization*, vol. 57, no. 1, pp. 57–78, 2008.
- [34] V. Berinde, *Iterative approximation of fixed points*. Springer, 2 ed., 2007.
- [35] A. Domahidi, A. U. Zraggen, M. N. Zeilinger, M. Morari, and C. N. Jones, "Efficient interior point methods for multistage problems arising in receding horizon control," in *IEEE Conference on Decision and Control*, (Maui, Hawaii, USA), pp. 668 – 674, 2012.
- [36] J. Mattingley and S. Boyd, "CVXGEN: a code generator for embedded convex optimization," *Optimization and Engineering*, vol. 13, no. 1, pp. 1–27, 2012.
- [37] H. J. Ferreau, H. G. Bock, and M. Diehl, "An online active set strategy to overcome the limitations of explicit MPC," *International Journal of Robust and Nonlinear Control*, vol. 18, no. 8, pp. 816–830, 2008.
- [38] M. Herceg, M. Kvasnica, C. N. Jones, and M. Morari, "Multi-parametric toolbox 3.0," in *European Control Conference*, (Zürich, Switzerland), pp. 502–510, 2013.

- [39] S. Merkli, J. L. Jerez, A. Domahidi, R. S. Smith, and M. Morari, “Circuit generation for efficient projection onto polyhedral sets in first-order methods,” in *European Control Conference*, (Linz, Austria), pp. 3440–3445, 2015.
- [40] H. H. Bauschke and P. L. Combettes, *Convex analysis and monotone operator theory in Hilbert spaces*. Springer, 2011.
- [41] J. Löfberg, “YALMIP : a toolbox for modeling and optimization in MATLAB,” in *Computer Aided Control Systems Design, IEEE International Symposium on*, (Taipei, Taiwan), pp. 284–289, Sept. 2004.
- [42] A. Liniger, A. Domahidi, and M. Morari, “Optimization-based autonomous racing of 1:43 scale RC cars,” *Optimal Control Applications and Methods*, vol. 36, no. 5, pp. 628–647, 2015.
- [43] A. B. Hempel, *Control of Piecewise Affine Systems Through Inverse Optimization*. PhD thesis, ETH Zürich, 2015. Dissertation, ETH-Zürich, 2015, No. 23222.
- [44] G. B. Dantzig, *Linear programming and extensions*. Princeton university press, 1963.